

1	General experimental methods .....	2
1.1	Synthesis.....	2
1.2	Spectroscopic studies .....	2
1.3	Electrochemical studies.....	3
1.4	Molecular modelling .....	4
1.5	Thermal analysis .....	4
1.6	Device fabrication and characterization.....	4
2	Synthetic procedures.....	5
	10-(2-bromophenyl)-10H-phenothiazine [QPTZ-Br].....	5
	2,7-dibromospiro[fluorene-9,9'-quinolino[3,2,1-kl]phenothiazine] [SQPTZ-2,7-FBr <sub>2</sub> ] ...	6
	spiro[fluorene-9,9'-quinolino[3,2,1-kl]phenothiazine]-2,7-diylbis(diphenylphosphine oxide) [SQPTZ-2,7-F(POPh <sub>2</sub> ) <sub>2</sub> ] .....	7
3	Thermal properties .....	8
4	Photophysical properties .....	9
5	Electrochemical studies .....	14
6	Molecular modelling .....	15
7	Single layer Phosphorescent OLED characteristics.....	24
8	Copy of NMR spectra .....	25
8.1	<b>SQPTZ-2,7-FBr<sub>2</sub></b> – <sup>1</sup> H – CD <sub>2</sub> Cl <sub>2</sub> .....	25
8.2	<b>SQPTZ-2,7-FBr<sub>2</sub></b> – <sup>13</sup> C – CD <sub>2</sub> Cl <sub>2</sub> .....	26
8.3	<b>SQPTZ-2,7-FBr<sub>2</sub></b> – <sup>13</sup> C – DEPT135 – CD <sub>2</sub> Cl <sub>2</sub> .....	27
8.4	<b>SQPTZ-2,7-F(POPh<sub>2</sub>)<sub>2</sub></b> – <sup>1</sup> H – CD <sub>2</sub> Cl <sub>2</sub> .....	28
8.5	<b>SQPTZ-2,7-F(POPh<sub>2</sub>)<sub>2</sub></b> – <sup>13</sup> C – CD <sub>2</sub> Cl <sub>2</sub> .....	29
8.6	<b>SQPTZ-2,7-F(POPh<sub>2</sub>)<sub>2</sub></b> – <sup>13</sup> C – DEPT 135 – CD <sub>2</sub> Cl <sub>2</sub> .....	30
8.7	<b>SQPTZ-2,7-F(POPh<sub>2</sub>)<sub>2</sub></b> – <sup>31</sup> P decoupled– CD <sub>2</sub> Cl <sub>2</sub> .....	31
9	Copy of high resolution mass spectroscopy spectra .....	32
10	References .....	34

## 1 General experimental methods

### 1.1 Synthesis

All manipulations of oxygen and moisture-sensitive materials were conducted with a standard Schlenk technique. All glassware was kept in an oven at a temperature of 80°C. Argon atmosphere was generated by three repetitive cycles of vacuum/Argon using a schlenck ramp. Commercially available reagents and solvents were used without further purification other than those detailed below. THF was obtained through a PURE SOLV™ solvent purification system. Light petroleum refers to the fraction with bp 40-60°C. Analytical thin layer chromatography was carried out using aluminum backed plates coated with Merck Kieselgel 60 GF254 and visualized under UV light (at 254 and 360 nm). Flash chromatography was carried out using Teledyne Isco CombiFlash® Rf 400 (UV detection 200-360nm), over standard silica cartridges (Redisep® Isco or Puriflash® columns Interchim).  $^1\text{H}$  and  $^{13}\text{C}$  NMR spectra were recorded using Bruker 300 MHz instruments ( $^1\text{H}$  frequency, corresponding  $^{13}\text{C}$  frequency: 75 MHz); chemical shifts were recorded in ppm and J values in Hz. The residual signals for the NMR solvents used are 5.32 ppm (proton) and 53.84 ppm (carbon) for  $\text{CD}_2\text{Cl}_2$ .<sup>[1]</sup> In the  $^{13}\text{C}$  NMR spectra, signals corresponding to C, CH, CH<sub>2</sub> or CH<sub>3</sub> groups, assigned from DEPT experiment, are noted. The following abbreviations have been used for the NMR assignment: s for singlet, d for doublet, t for triplet, q for quadruplet and m for multiplet. High resolution mass spectra were recorded at the Centre Régional de Mesures Physiques de l'Ouest (CRMPO-Rennes) on a Thermo Fisher Q-Exactive instrument or a Bruker MaXis 4G or a Bruker Ultraflex III.

### 1.2 Spectroscopic studies

Cyclohexane (spectroscopic grade, Acros), THF (spectroscopic grade, Merck), dichloromethane (spectroscopic grade, Acros), methanol (spectroscopic grade, Acros), Acetonitrile (spectroscopic grade, Acros), 2-MeTHF (Anhydrous, >99 %, Sigma Aldrich), 1 N solution of sulfuric acid in water (Standard solution, Alfa Aesar) and quinine sulfate dihydrate (99+%, ACROS organics) were used without further purification.

UV-visible spectra were recorded using an UV-Visible spectrophotometer SHIMADZU UV-1605. Molar extinction coefficients ( $\epsilon$ ) were calculated from the gradients extracted from the plots of absorbance vs concentration with five solutions of different concentrations for each sample.

$$A = \epsilon \times l \times C$$

Emission spectra and phosphorescence decay were recorded with a HORIBA Scientific Fluoromax-4 equipped with a Xenon lamp. Singlet and triplet energy levels were calculated from the onset of the fluorescence spectrum at RT and from the maximum of the first phosphorescence emission peak at 77 K respectively. Conversion in electron-volt was obtained

$$\text{with the following formula: } E_{S \text{ or } T}(\text{eV}) = \frac{hc}{\lambda} \text{ with } h = 6.62607 \times 10^{-34} \text{ J.s}, C = 2.99792 \times 10^{17} \text{ nm.s}^{-1}$$

$$\text{and } 1 \text{ J} = 1.60218 \times 10^{-19} \text{ eV. This equation can be simplified as: } E_T(\text{eV}) = \frac{1239.84}{\lambda} \text{ with } \lambda \text{ formulated in nm.}$$

Quantum yields in solution ( $\Phi_{\text{sol}}$ ) were calculated relative to quinine sulfate ( $\Phi_{\text{ref}} = 0.546$  in  $\text{H}_2\text{SO}_4$  1 N).  $\Phi_{\text{sol}}$  was determined according to the following equation,

$$\phi_{\text{sol}} = \phi_{\text{ref}} \times \frac{\text{Grad}_s}{\text{Grad}_r} \times \left(\frac{\eta_s}{\eta_r}\right)^2$$

where subscripts  $s$  and  $r$  refer respectively to the sample and reference,  $\text{Grad}$  is the gradient from the plot of integrated fluorescence intensity vs absorbance,  $\eta$  is the refracting index of the solvent ( $\eta_s = 1.426$  for cyclohexane). Five solutions of different concentration ( $A < 0.1$ ) of the sample and five solutions of the reference (quinine sulfate) were prepared. The integrated area of the fluorescence peak was plotted against the absorbance at the excitation wavelength for both the sample and reference. The gradients of these plots were then injected in the equation to calculate the reported quantum yield value for the sample.

Low temperature (77 K) measurements were performed in 2-MeTHF which freezes as a transparent glassy matrix. Measurements were carried in a single block quartz tube containing the solution, which was placed in an oxford Optistat Cryostat cooled with liquid nitrogen.

Lipper-Mataga-Ooshika formalism<sup>[2][3][4]</sup> was used to estimate the excited state dipole moment.

$$\Delta\nu = \frac{2(\Delta\mu)^2}{r^3hc} \Delta f + C \text{ with } \Delta f = \left( \frac{\varepsilon - 1}{2\varepsilon + 1} - \frac{n^2 - 1}{n^2 + 1} \right)$$

With  $\Delta\nu$  ( $\text{cm}^{-1}$ ) being the Stokes shift,  $\Delta\mu$  (D) the dipole moment difference between  $S_0$  and  $S_1$  states,  $r$  (cm) the radius of the solvation sphere obtained from geometry optimisation at the ground state (DFT b3lyp 6-31g(d)),  $h$  the Planck constant ( $6.626 \cdot 10^{-34} \text{ m}^2 \cdot \text{kg} \cdot \text{s}^{-1}$ ),  $c$  the celerity ( $2,998 \times 10^8 \text{ m.s}^{-1}$ ),  $\Delta f$  the orientation polarisability of the solvent calculated from its dielectric constant  $\varepsilon$  ( $\text{F.m}^{-1}$ ) and its refractive index  $n$ , and  $C$  a constant.

Experimentally,  $\Delta\nu$  were calculated from the maximal wavelength in absorption and emission spectra measured in five different solvents (Cyclohexane, dichloromethane, tetrahydrofuran, methanol and acetonitrile).  $\Delta f$  were calculated from  $\varepsilon$  and  $n$  for the five different solvents. Then,  $\Delta f$  as a function of  $\Delta\nu$  was plotted and the slope is calculated using a linear regression. Finally,  $\Delta\mu$  is calculated as follow:

$$\Delta\mu = \sqrt{\frac{r^3hc.\text{slope}}{2}}$$

Excited state dipole moment  $\mu^*$  is then calculated from the ground state dipole moment  $\mu$  estimated by DFT calculations and  $\Delta\mu$ .

Infrared spectra were recorded on a Bruker Vertex 7 0 using a diamond crystal MIRacle ATR (Pike).

### 1.3 Electrochemical studies

Electrochemical experiments were performed under argon atmosphere using a Pt disk electrode (diameter 1 mm). The counter electrode was a vitreous carbon rod. The reference electrode was either a silver wire in a 0.1 M  $\text{AgNO}_3$  solution in  $\text{CH}_3\text{CN}$  for the studies in oxidation or a Silver wire coated by a thin film of  $\text{AgI}$  (silver(I)iodide) in a 0.1 M  $\text{Bu}_4\text{NI}$  solution in DMF for the

studies in reduction. Ferrocene was added to the electrolyte solution at the end of a series of experiments. The ferrocene/ferrocenium ( $\text{Fc}/\text{Fc}^+$ ) couple served as internal standard. The three electrodes cell was connected to a PAR Model 273 potentiostat/galvanostat (PAR, EG&G, USA) monitored with the ECHEM Software. Activated  $\text{Al}_2\text{O}_3$  was added in the electrolytic solution to remove excess moisture. For a further comparison of the electrochemical and optical properties, all potentials are referred to the SCE electrode that was calibrated at  $-0.405 \text{ V}$  vs.  $\text{Fc}/\text{Fc}^+$  system. Following the work of Jenekhe,<sup>[5]</sup> we estimated the electron affinity (EA) or lowest unoccupied molecular orbital (LUMO) and the ionization potential (IP) or highest occupied molecular orbital (HOMO) from the redox data. The LUMO level was calculated from the cyclic voltammetry in reduction as follow:  $\text{LUMO (eV)} = -[\text{E}_{\text{onset}} \text{ (vs SCE)} + 4.4]$ . Similarly the HOMO level was calculated from the cyclic voltammetry in oxydation as follow:  $\text{HOMO (eV)} = -[\text{E}_{\text{onset}} \text{ (vs SCE)} + 4.4]$  based on an SCE energy level of 4.4 eV relative to the vacuum. The electrochemical gap was calculated from:  $\Delta E^{\text{el}} = |\text{HOMO-LUMO}| \text{ (in eV)}$ .

#### 1.4 Molecular modelling

Full geometry optimization of the ground state and vibrational frequency calculation were performed with Density Functional Theory (DFT)<sup>[6]</sup> using the hybrid Becke-3 parameter exchange functional<sup>[7]</sup> and the Lee-Yang-Parr non-local correlation functional<sup>[8]</sup> (B3LYP) implemented in the Gaussian 16 program suite,<sup>[9]</sup> using the 6-31G(d) basis set and the default convergence criterion implemented in the program. All stationary points were characterized as minima by analytical frequency calculations.

Optical transition diagrams were obtained through TD-DFT calculations performed using the B3LYP functionals and the 6-311+G(d,p) basis set from the geometry of  $S_0$ .

Calculations were carried out on the OCCIGEN calculator of the Centre Informatique National de l'Enseignement Supérieur (CINES (Montpellier) under project N° 2021-A0100805032).

#### 1.5 Thermal analysis

Thermal Gravimetric Analysis (TGA) was carried out by using a Mettler-Toledo TGA-DSC-1 apparatus. TGA curved were measured at  $10^\circ\text{C}/\text{min}$  from  $30^\circ\text{C}$  to  $1000^\circ\text{C}$  under a nitrogen flux. Differential Scanning Calorimetry (DSC) was carried out by using a NETZSCH DSC 200 F3 instrument equipped with an intracooler DSC traces were measured at  $10^\circ\text{C}/\text{min}$ , 2 heating/cooling cycles were successively carried out under a nitrogen flux.

#### 1.6 Devices fabrication and characterization

*Single layer phosphorescent organic light emitting diodes (SL-PhOLEDs)*

The structure of the SL devices is the following: ITO/PEDOT:PSS (40 nm)/Emissive layer *host:guest* 10 % (100 nm)/LiF (1.2 nm)/Al (100 nm). In this devices, ITO/PEDOT:PSS (Poly(3,4-ethylenedioxythiophene)-poly(styrenesulfonate)) is used as the anode and a thin film of lithium fluoride covered with aluminum is the cathode. The devices have been fabricated onto patterned ITO coated glass substrates from XinYan Tech (thickness: 100 nm and sheet resistance: less of 20 W/m). The organic materials are deposited onto the ITO anode by sublimation under high vacuum ( $< 10^{-6} \text{ Torr}$ ) at a rate of 0.2 – 0.3 nm/s. The entire device is fabricated in the same run without breaking the vacuum. In this study, the thicknesses of the

different organic layers were kept constant for all the devices. The active area of the devices defined by the overlap of the ITO anode and the metallic cathode was 0.3 cm<sup>2</sup>. The current-voltage-luminance (I-V-L) characteristics of the devices were measured with a regulated power supply (Laboratory Power Supply EA-PS 3032-10B) combined with a multimeter and a 1 cm<sup>2</sup> area silicon calibrated photodiode (Hamamatsu). The spectral emission was recorded with a SpectraScan PR650 spectrophotometer. All the measurements were performed at room temperature and at ambient atmosphere with no further encapsulation of devices.

#### *Space-charged limited current (SCLC) diodes*

Solution preparation conditions: All four investigated molecules were dissolved in chloroform (CHCl<sub>3</sub>) to form solutions with same concentrations of 60 mg/ml. Well-sealed vials with prepared solutions were left stirring at room temperature for at least 3 hours prior to spin-coating.

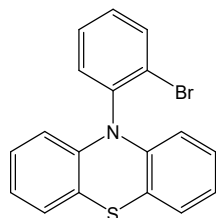
Fabrication of hole-only space-charge limited current (SCLC) diodes: Indium-tin oxide (ITO) coated glass was used as a substrate. A sequential cleaning of the substrates in soap water, distilled water, acetone and isopropanol (15 min for each step) using ultrasonic bath was performed. A thin, highly conductive poly(ethylenedioxythiophene):polystyrene sulfonate (PEDOT:PSS) layer was spin-coated onto pre-cleaned ITO and used as a bottom electrode. Then samples were transferred into a nitrogen-filled glove box system and thermally annealed at 140°C for 30 min. After that, all the investigated layers were spin-coated at 600 rpm for 80 sec to obtain homogeneous thin films. Spin-coated samples were placed into a vacuum chamber and left overnight under high vacuum ( $\approx 5 \times 10^{-7}$  mbar). SCLC devices were completed by sequential thermal evaporation of MoO<sub>3</sub> (7nm) and Ag (250 nm) layers.

Fabrication of electron-only space-charge limited current (SCLC) diodes: Identical ITO substrates and cleaning conditions were applied as for hole-only samples (see above). A thin ZnO layer (20-25 nm) was spin-coated onto pre-cleaned ITO and thermally annealed at 110°C for 15 min and used as a bottom contact. After deposition of the molecules by spin-coating and placing into a vacuum chamber, devices were completed by a sequential evaporation of Ca (20 nm) and Al (300 nm) as a top contact.

SCLC diode current-voltage characteristics were measured, inside the glove-box, using Keithley semiconductor characterization system 4200. The active-layer thicknesses were measured after SCLC characterization using a profilometer.

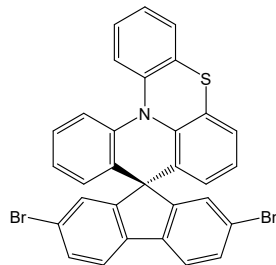
## 2 Synthetic procedures

### 10-(2-bromophenyl)-10H-phenothiazine [QPTZ-Br]



Phenothiazine (2.00 g, 10.1 mmol, 1.0 eq), 1-bromo-2-iodobenzene (2.84 g, 1.29 mL, 10.1 mmol, 1 eq), Cu<sub>2</sub>O (0.290 g, 2.0 mmol, 0.2 eq), K<sub>3</sub>PO<sub>4</sub> (6.40 g, 30.3 mmol, 3 eq) and N,N,N,N-tetramethylethylenediamine ( $1.17 \times 10^{-4}$  g, 0.15 mL, 1.0 mmol, 0.1 eq) were dissolved in *o*-dichlorobenzene (30 mL). The resulting mixture was refluxed under argon atmosphere for 36 h. The reaction mixture was concentrated under reduced pressure. The crude was dissolved in CH<sub>2</sub>Cl<sub>2</sub> (30 mL) and water was added (100 mL). The organic layer was extracted with CH<sub>2</sub>Cl<sub>2</sub> (4 × 30mL), washed with water (3 × 40 mL), brine (1 × 40 mL) and finally dried over MgSO<sub>4</sub>. Solvent was then evaporated under reduced pressure and the crude product was purified by flash chromatography on silica gel [column conditions: silica cartridge (40 g); solid deposit on Celite®; λ<sub>detection</sub>: (254 nm, 280 nm); gradient CH<sub>2</sub>Cl<sub>2</sub>/light petroleum from 0 to 10% in 50 min at 40 mL/min], a pale yellow solid was obtained (2.57 g, 7.25 mmol); yield 72 %. <sup>1</sup>H NMR (300 MHz, CDCl<sub>3</sub>): δ 7.86 (dd, J = 8.0, 1.4 Hz, 1H), 7.60 – 7.48 (m, 2H), 7.38 (m, 1H), 7.01 – 6.96 (m, 2H), 6.87 – 6.76 (m, 4H), 6.04 – 6.00 (m, 2H). m.p.: 86 °C see litt. [10]

### 2,7-dibromospiro[fluorene-9,9'-quinolino[3,2,1-kl]phenothiazine] [SQPTZ-2,7-FBr<sub>2</sub>]



1<sup>st</sup> step: **QPTZ-Br** (1.90 g, 5.33 mmol, 1.2 eq) in dry THF (60 mL) under argon and the mixture was cooled to -78°C. *n*-BuLi (2.50 M in hexanes, 2.13 mL, 5.33 mmol, 1.2 eq) was then added dropwise and the resulting mixture was stirred for 30 min. 2,7-dibromofluorenone (1.50 g, 4.44 mmol, 1.0 eq) dissolved in dry THF (15 mL) at -78°C was added dropwise to the reaction mixture and stirred for 30 additional minutes. Then, the reaction was allowed to warm up to room temperature under stirring overnight. Solvent was removed under reduced pressure and the crude was dried under vacuum at 60°C for 2 hours.

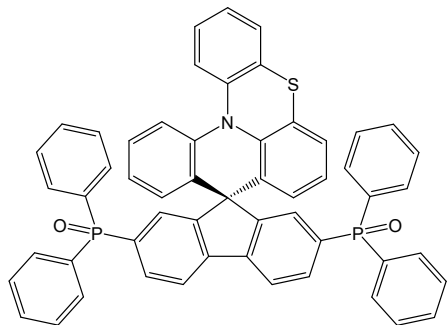
2<sup>nd</sup> step: Without further purification, the crude was dissolved in acetic acid (80 mL) and hydrochloric acid (8 mL) was added under stirring. The reaction mixture was refluxed for 5 hours under stirring.

After cooling to room temperature, water was added to the reaction mixture. The precipitate was filtered off and then dissolved in CH<sub>2</sub>Cl<sub>2</sub>. The organic layer was washed with water and dried over MgSO<sub>4</sub>. Solvent was then removed under reduced pressure. A hot saturated solution of the crude in CHCl<sub>3</sub> was prepared and the product was precipitated by adding MeOH. This was repeated several times. Product was finally dried under vacuum at 40°C overnight.

The *title compound* was obtained as a white solid (1.78 g, 2.99 mmol); yield 56%; <sup>1</sup>H (300 MHz, CD<sub>2</sub>Cl<sub>2</sub>) δ 7.78 (d, J = 8.2 Hz, 1H), 7.70 (d, J = 8.2 Hz, 1H), 7.61 – 7.48 (m, 3H), 7.45 – 7.12 (m, 8H), 6.93 – 6.79 (m, 2H), 6.55 (d, J = 7.9 Hz, 1H), 6.38 (d, J = 7.9 Hz, 1H) ppm. <sup>13</sup>C NMR (75 MHz, CD<sub>2</sub>Cl<sub>2</sub>): δ 155.8 (C), 152.4(C), 143.3 (C), 141.2 (C), 139.6 (C), 139.5 (C), 135.8 (C), 132.5 (CH), 132.0 (C), 131.5 (CH), 130.7 (CH), 129.7 (C), 129.2 (CH), 128.5 (CH),

128.4 (CH), 127.8 (CH), 127.5 (C), 127.3 (2CH), 126.8 (CH), 125.4 (CH), 125.3 (C), 124.8 (CH), 124.6 (CH), 122.9 (C), 122.7 (C), 122.5 (CH), 122.4 (CH), 120.7 (CH), 119.3 (CH), 57.9 (C) ppm. IR (ATR, platinum): 3060, 1920, 1884, 1781, 1737, 1706, 1591, 1579, 1568, 1541, 1489, 1475, 1455, 1434, 1410, 1394, 1325, 1317, 1294, 1272, 1249, 1232, 1211, 1189, 1161, 1134, 1119, 1101, 1082, 1058, 1035, 1005, 994, 980, 960, 939, 914, 870, 853, 829, 806, 795, 781, 768, 754, 744, 730, 721, 698, 675, 655, 640, 621, 604, 580, 549, 534, 526, 514, 504, 484, 454, 439 cm<sup>-1</sup>. HRMS (ASAP, 230 °C): Found [M+H]<sup>+</sup> 593.9522; C<sub>31</sub>H<sub>18</sub>NBr<sub>2</sub>S required 593.95212. m.p.: 311°C.

spiro[fluorene-9,9'-quinolino[3,2,1-kl]phenothiazine]-2,7-diylbis(diphenylphosphine oxide) **[SQPTZ-2,7-F(POPh<sub>2</sub>)<sub>2</sub>]**



1<sup>st</sup> step: **SQPTZ-2,7-FBr<sub>2</sub>** (0.400 g, 0.672 mmol, 1.0 eq) in dry THF (30 mL) was dissolved in dry THF (30 mL) under argon. The reaction mixture was then cooled to -78°C and *n*-BuLi (2.50 M in hexanes, 0.64 mL, 1.61 mmol, 2.4 eq) was added dropwise. The reaction mixture was stirred for 2 hours at -78°C. Chlorodiphenylphosphine (0.055 g, 0.64 mL, 1.61 mmol, 2.5 eq) was then added and stirred for 2 additional hours at -78°C. The reaction mixture was finally allowed to warm up to room temperature under stirring overnight. The reaction mixture was quenched with few drops of absolute ethanol and concentrated under reduced pressure. The crude product was dissolved in CH<sub>2</sub>Cl<sub>2</sub>. The organic layer was washed with water, brine, dried over MgSO<sub>4</sub> and filtered. Solvent was removed under reduced pressure and dried under vacuum at 60°C for 5 hours.

2<sup>nd</sup> step: Without any further purification, the crude was dissolved in CH<sub>2</sub>Cl<sub>2</sub> (30 mL) and H<sub>2</sub>O<sub>2</sub> (3 mL, 35 wt. % in water) was added to the mixture which was stirred overnight at room temperature. The organic layer was washed several times with water and dried over MgSO<sub>4</sub>. Solvent was then evaporated under reduced pressure and the crude was purified with flash chromatography on silica gel.

After purification flash chromatography on silica gel [column condition: silica cartridge (40 g); solid deposit on Celite®; λdetection: (254 nm, 280 nm); gradient CH<sub>2</sub>Cl<sub>2</sub>/CH<sub>3</sub>OH from 100 to 95% in 40 min at 40 mL/min], a pale green solid was obtained (0.465 g, 0.554 mmol); yield 82%. <sup>1</sup>H NMR (300 MHz, CD<sub>2</sub>Cl<sub>2</sub>) δ 7.77 (d, *J* = 8.2 Hz, 2H), 7.70 (d, *J* = 8.2 Hz, 2H), 7.62 – 7.47 (m, 8H), 7.46 – 7.11 (m, 17H), 6.89 (t, *J* = 7.6, 2H), 6.82 (t, *J* = 7.7 Hz, 2H), 6.56 (d, *J* = 8.0 Hz, 2H), 6.38 (d, *J* = 7.9 Hz, 2H) ppm. <sup>13</sup>C NMR (75 MHz, CD<sub>2</sub>Cl<sub>2</sub>) δ 154.9 (C), 154.7 (C), 151.6 (C), 151.4 (C), 145.4 (C), 142.6 (C), 140.2 (C), 139.5 (C), 139.2 (C), 135.5 (C), 134.6 (C), 134.3 (C), 134.0 (C), 133.3 (CH), 133.2 (CH), 132.9 (CH), 132.7 (CH), 132.5 (CH), 132.5 (4CH), 132.4 (2CH), 132.2 (CH), 132.1 (CH), 132.0 (CH), 131.8 (C), 131.4 (CH), 131.3 (CH),

129.5 (C), 129.2 (2CH), 129.0 (2CH), 129.0 (CH), 128.9 (CH), 128.9 (CH), 128.8 (CH), 128.4 (CH), 127.9 (CH) 127.8 (CH), 127.1 (CH), 127.0 (C), 126.6 (CH), 125.1 (CH), 125.0 (C), 124.8 (CH), 124.6 (CH), 124.4(CH), 121.8 (CH), 121.6 (CH), 120.5(CH), 119.1 (CH), 58.1 (C) ppm.  $^{31}\text{P}$  NMR (121 MHz,  $\text{CD}_2\text{Cl}_2$ )  $\delta$  27.01, 25.72 ppm. IR (ATR, platinum): 3674, 3407, 3052, 2360, 1650, 1602, 1588, 1571, 1560, 1490, 1478, 1455, 1436, 1395, 1330, 1319, 1297, 1272, 1252, 1231, 1188, 1159, 1133, 1118, 1101, 1073, 1038, 1026, 1000, 972, 955, 941, 920, 894, 868, 857, 834, 819, 791, 780, 770, 750, 725, 712, 691, 647, 623, 609, 584, 561, 550, 537, 525, 497, 482, 451, 443, 431  $\text{cm}^{-1}$ . HRMS (ASAP, 325 °C): Found [M+H] $^+$ , 838.2094;  $\text{C}_{55}\text{H}_{38}\text{NO}_2\text{P}_2\text{S}$  required 838.2093. m.p.: 236 °C.

### 3 Thermal properties

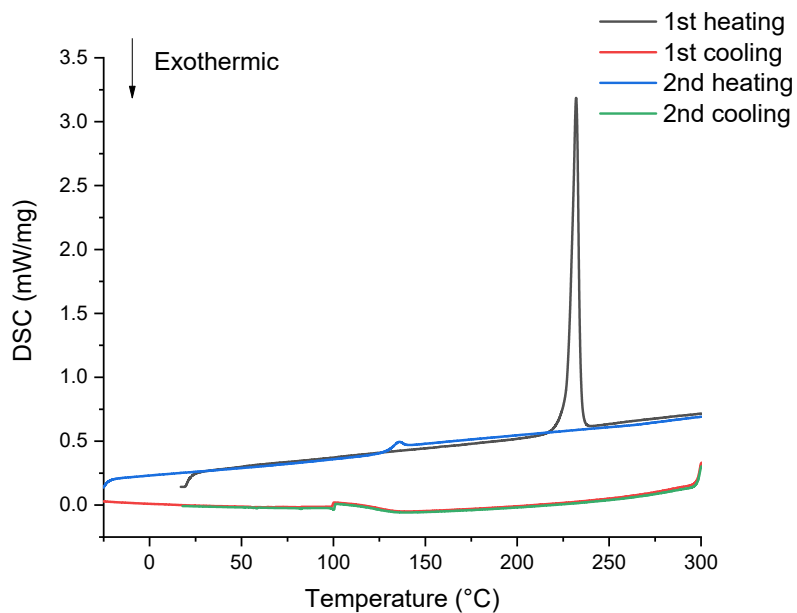


Figure S 1 DSC curves of **SQPTZ-F**

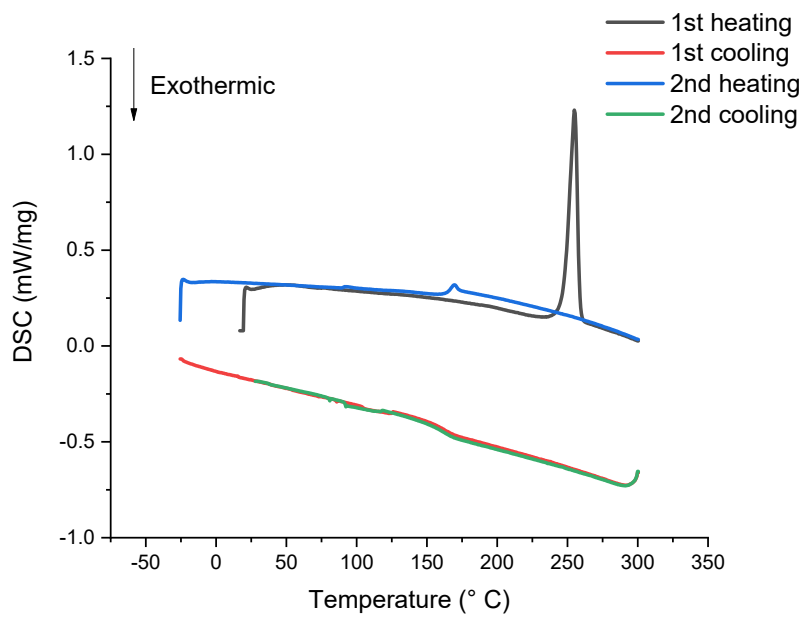


Figure S 2 DSC curves of **SQPTZ-2,7-F(POPh<sub>2</sub>)<sub>2</sub>**

#### 4 Photophysical properties

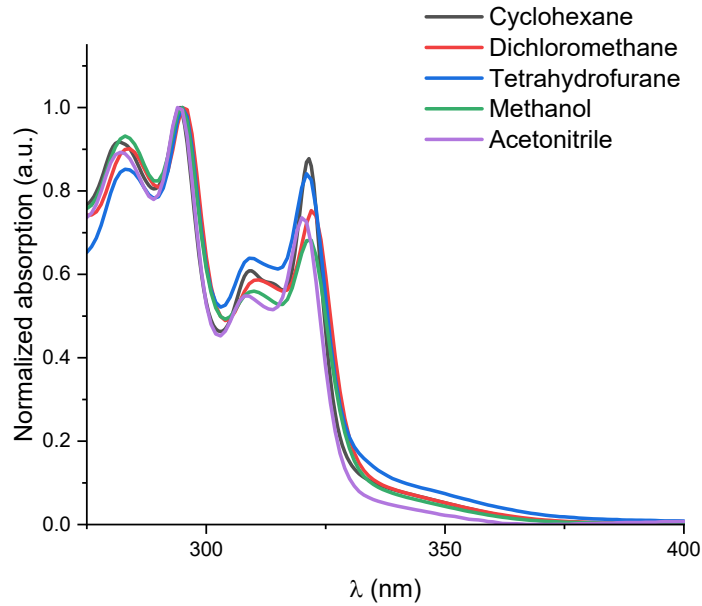


Figure S 3 Absorption spectra of **SQPTZ-2,7-F(POPh<sub>2</sub>)<sub>2</sub>** in various solvents

Table S 2 Lippert-Mataga formalism calculation of **SQPTZ-2,7-F(POPh<sub>2</sub>)<sub>2</sub>** in various solvents

solvent	$\lambda_{\text{abs}}$ (nm)	$\lambda_{\text{em}}$ (nm)	$\nu_{\text{abs}}$ (cm <sup>-1</sup> )	$\nu_{\text{em}}$ (cm <sup>-1</sup> )	$\Delta\nu$ (cm <sup>-1</sup> )	$\epsilon$ (F.m <sup>-1</sup> )	n	$\Delta f$
cyclohexane	321	452	31152.65	22123.89381	9028.754	2.02	1.426	-0.00158
DCM	322	536	31055.9	18656.71642	12399.18	8.93	1.424	0.21717
THF	321	520	31152.65	19230.76923	11921.88	7.58	1.407	0.20964
ACN	320	574	31250	17421.60279	13828.4	37.5	1.344	0.305454
methanol	322	591	31055.9	16920.47377	14135.43	37.2	1.328	0.311439

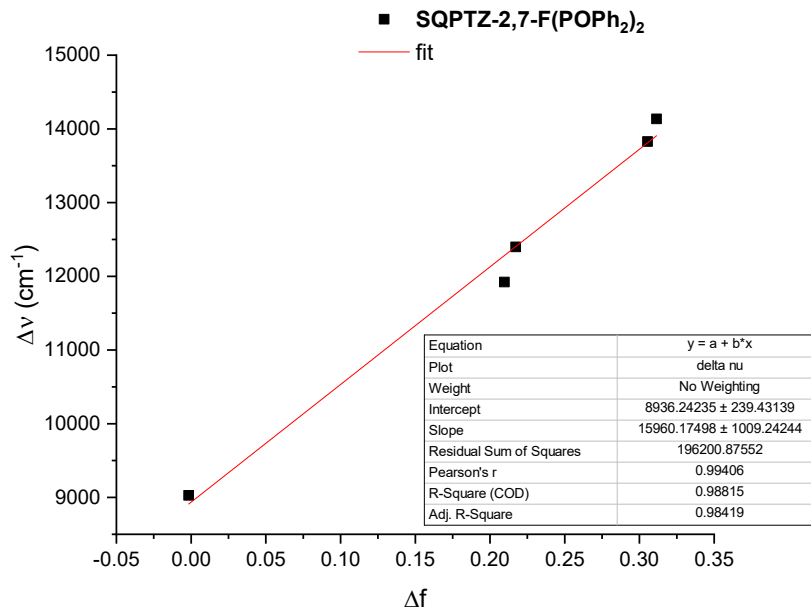


Figure S 4 Lippert-Mataga formalism linear fit for **SQPTZ-2,7-F(POPh<sub>2</sub>)<sub>2</sub>**

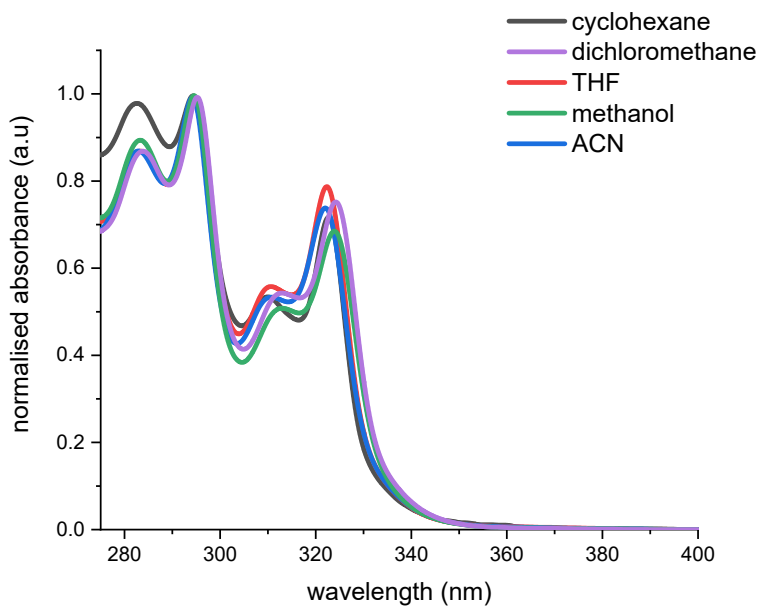


Figure S 5 Absorption spectra of **SPA-2,7-F(POPh<sub>2</sub>)<sub>2</sub>** in various solvents

Table S 3 Lippert-Mataga formalism calculation of **SPA-2,7-F(POPh<sub>2</sub>)<sub>2</sub>** in various solvents

solvent	$\lambda_{\text{abs}}$ (nm)	$\lambda_{\text{em}}$ (nm)	$v_{\text{abs}}$ (cm <sup>-1</sup> )	$v_{\text{em}}$ (cm <sup>-1</sup> )	$\Delta v$ (cm <sup>-1</sup> )	$\varepsilon$ (F.m <sup>-1</sup> )	n	$\Delta f$
cyclohexane	322.5	439	31007.75194	22779.04328	8228.7087	2.02	1.426	-0.00158
dichloromethane	324	496	30864.19753	20161.29032	10702.907	8.93	1.424	0.21717
THF	322	486	31055.90062	20576.13169	10479.769	7.58	1.407	0.20964
ACN	322	525	31055.90062	19047.61905	12008.282	37.5	1.344	0.305454
methanol	324	538	30864.19753	18587.36059	12276.837	37.2	1.328	0.311439

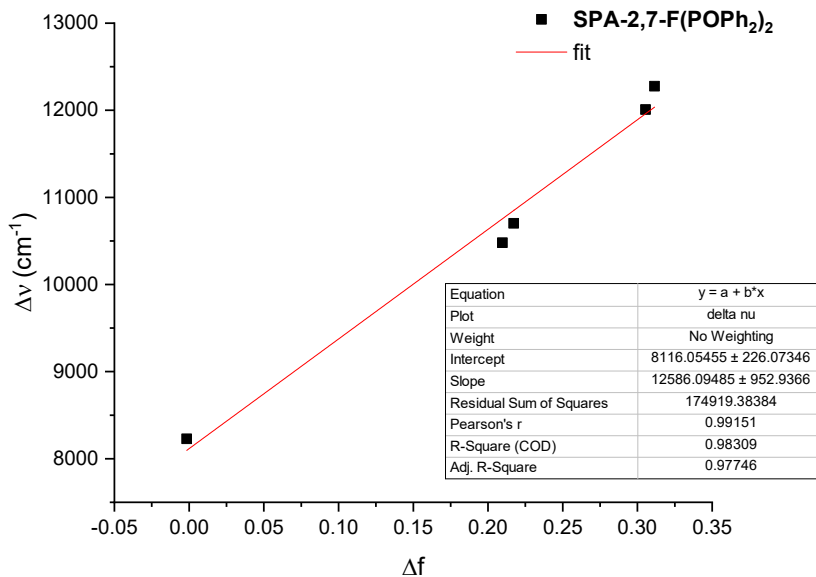


Figure S 6 Lippert-Mataga formalism linear fit for **SPA-2,7-F(POPh<sub>2</sub>)<sub>2</sub>**

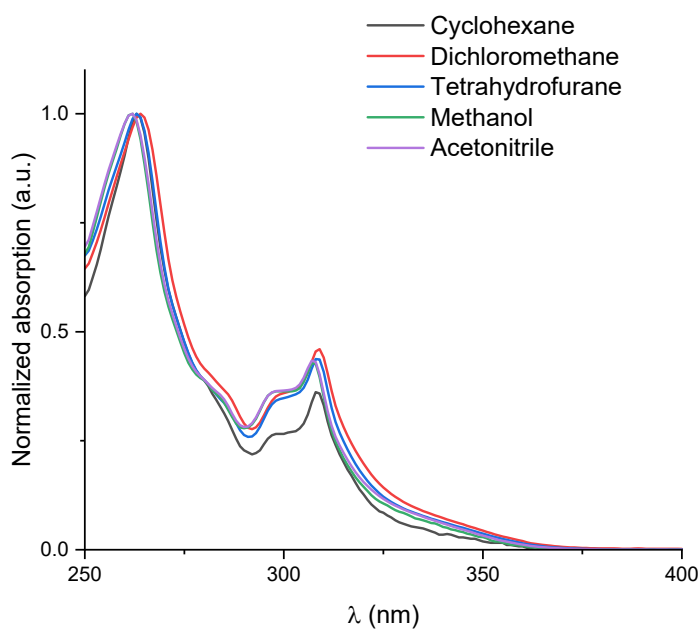


Figure S 7 Absorption spectra of **SQPTZ-F** in various solvents

Table S 4 Lippert-Mataga formalism calculation of **SQPTZ-F** in various solvents

solvent	$\lambda_{\text{abs}}$ (nm)	$\lambda_{\text{em}}$ (nm)	$\nu_{\text{abs}}$ (cm $^{-1}$ )	$\nu_{\text{em}}$ (cm $^{-1}$ )	$\Delta\nu$ (cm $^{-1}$ )	$\epsilon$ (F.m $^{-1}$ )	$n$	$\Delta f$
<b>cyclohexane</b>	309	417	32362.46	23980.82	8381.644	2.02	1.426	-0.00158
<b>DCM</b>	309	420	32362.46	23809.52	8552.936	8.93	1.424	0.21717
<b>THF</b>	309	420	32362.46	23809.52	8552.936	7.58	1.407	0.20964
<b>ACN</b>	308	419	32467.53	23866.35	8601.184	37.5	1.344	0.305454
<b>methanol</b>	308	419	32467.53	23866.35	8601.184	37.2	1.328	0.311439

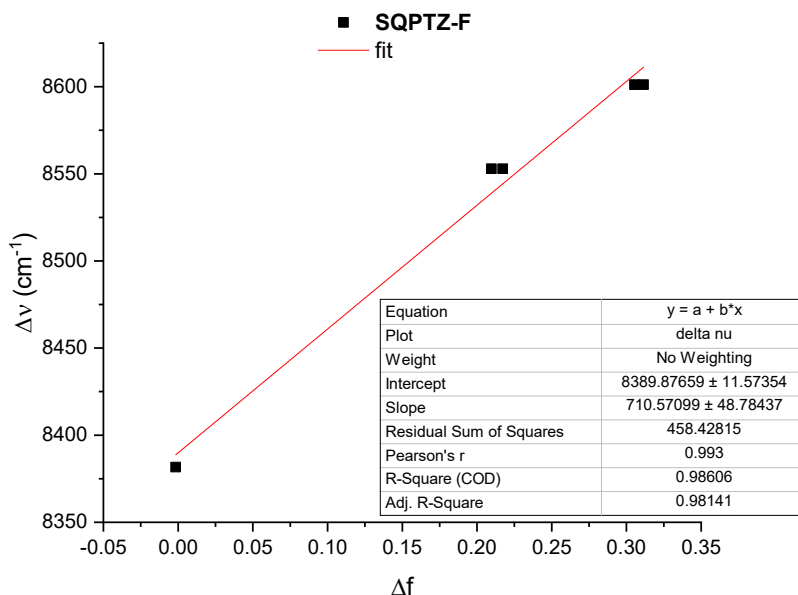


Figure S 8 Lippert-Mataga formalism linear fit for **SQPTZ-F**

Table S 5 Summary of the radius of the solvation sphere ( $r$ ), dipole moment at the ground ( $\mu$ ) and excited ( $\mu^*$ ) states and the difference ( $\Delta\mu$ ) for **SQPTZ-2,7-F(POPh<sub>2</sub>)<sub>2</sub>**, **SPA-2,7-F(POPh<sub>2</sub>)<sub>2</sub>** and **SQPTZ-F**.

Compound	$r$ (Å)	$\Delta\mu$ (D)	$\mu$ (D)	$\mu^*$ (D)
<b>SQPTZ-2,7-F(POPh<sub>2</sub>)<sub>2</sub></b>	18.1	34.2	5.9	40.1
<b>SPA-2,7-F(POPh<sub>2</sub>)<sub>2</sub></b>	18.4	31.2	9.3	40.5
<b>SQPTZ-F</b>	11.1	3.5	1.5	5.0

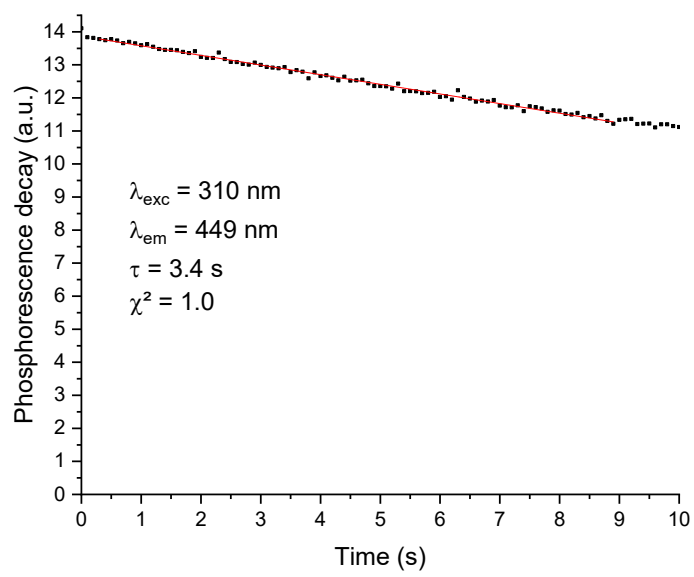


Figure S 9 Phosphorescence decay of **SQPTZ-2,7-F(POPh<sub>2</sub>)<sub>2</sub>** in a frozen matrix of 2-MeTHF at 77K

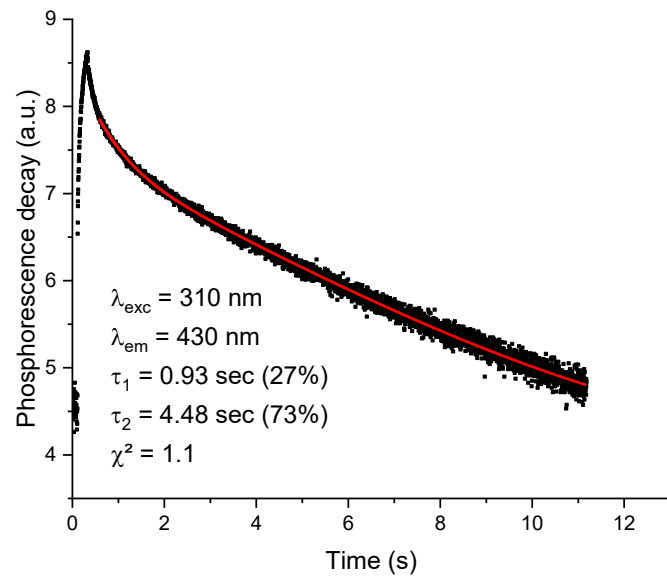


Figure S 10 Phosphorescence decay of **SQPTZ-F** in a frozen matrix of 2-MeTHF at 77K

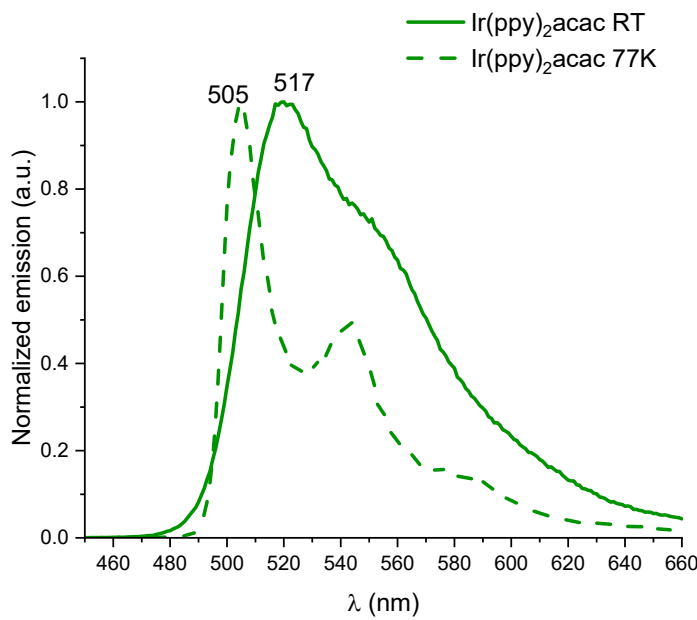


Figure S 11 Normalized emission spectra of  $\text{Ir}(\text{ppy})_2\text{acac}$  in 2-MeTHF at RT (solid line) and at 77 K (dashed line),  $\lambda_{\text{exc}} = 415 \text{ nm}$ .

## 5 Electrochemical studies

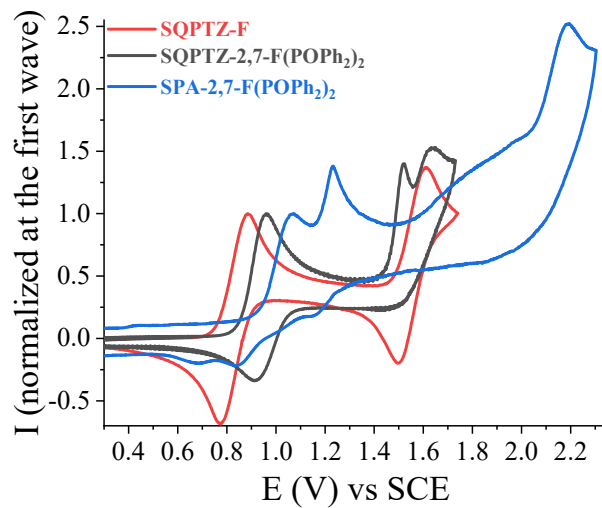


Figure S 12 Cyclic voltammetry in  $\text{CH}_2\text{Cl}_2 + \text{Bu}_4\text{NPF}_6$  0.2 M, sweep-rate 100  $\text{mV.s}^{-1}$  of **SQPTZ-2,7-F(POPh<sub>2</sub>)<sub>2</sub>**, **SQPTZ-F** and **SPA-2,7-F(POPh<sub>2</sub>)<sub>2</sub>**

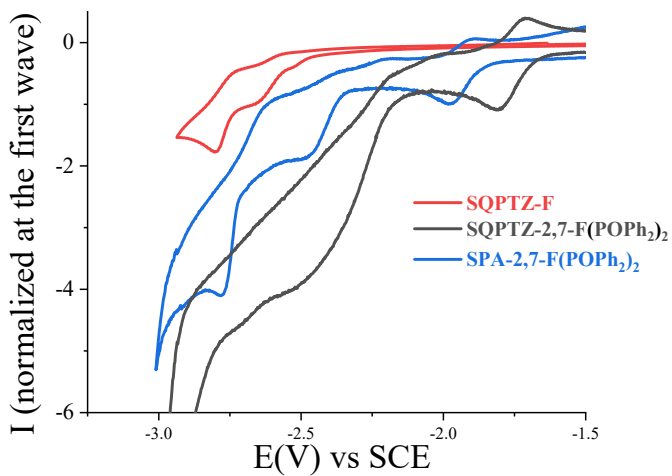


Figure S 13 Cyclic voltammetry in  $DMF + Bu_4NPF_6\ 0.1\ M$ , sweep-rate  $100\ mV.s^{-1}$ ) of **SQPTZ-2,7-F(POPh<sub>2</sub>)<sub>2</sub>**, **SQPTZ-F** and **SPA-2,7-F(POPh<sub>2</sub>)<sub>2</sub>**

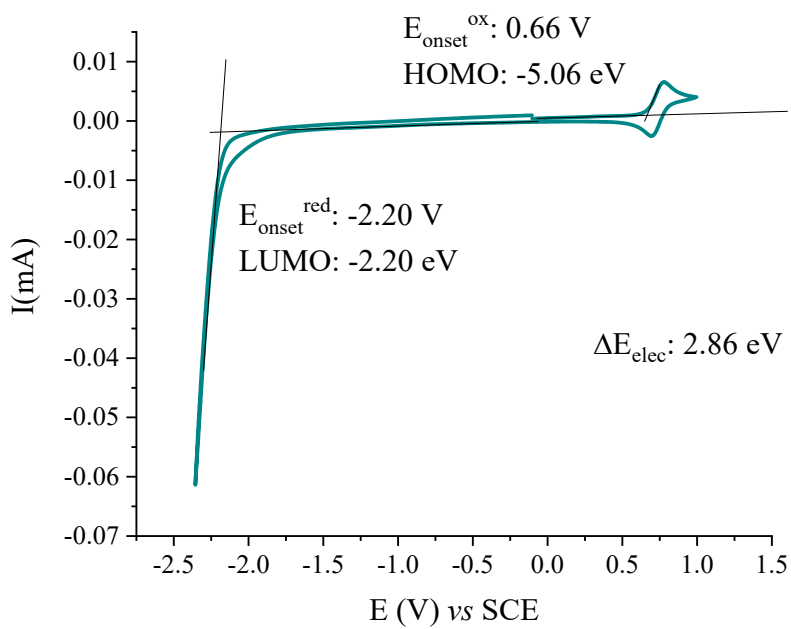


Figure S 14 Cyclic voltammetry in  $CH_2Cl_2 + Bu_4NPF_6\ 0.2\ M$ , sweep-rate  $100\ mV.s^{-1}$  of  $Ir(ppy)_2acac$ .

## 6 Molecular modelling

Table S 6 Results of TD-DFT calculations for **SQPTZ-F**

Wavelength (nm)	Oscillator Strength	Major contributions
359	0.002	HOMO→LUMO (96%)
345	0.027	HOMO→L+1 (80%), HOMO→L+2 (15%)
336	0.003	HOMO→L+1 (14%), HOMO→L+2 (34%),

		HOMO→L+3 (44%)
322	0.043	HOMO→L+2 (46%), HOMO→L+3 (45%)
308	0.119	HOMO→L+4 (62%), HOMO→L+5 (28%)
305	0.024	HOMO→L+4 (30%), HOMO→L+5 (61%)
292	0.069	H-1→LUMO (78%)
287	0.054	HOMO→L+6 (85%)
282	0.015	H-2→LUMO (47%), H-1→L+1 (23%), H-1→L+2 (10%)
279	0.117	H-2→LUMO (43%), H-1→L+1 (38%)
271	0.055	H-2→L+1 (42%), H-1→L+1 (18%), H-1→L+2 (22%)
269	0.013	H-2→L+1 (32%), H-1→L+2 (40%), HOMO→L+7 (10%)

Table S 7 Results of TD-DFT calculations for **SQPTZ-2,7-F(POPh<sub>2</sub>)<sub>2</sub>**

Wavelength (nm)	Oscillator Strength	Major contributions
432	0.001	HOMO→LUMO (99%)
358	0.015	HOMO→L+1 (80%), HOMO→L+3 (14%)
342	0.010	HOMO→L+3 (13%), HOMO→L+5 (67%)
335	0.000	HOMO→L+2 (85%)
332	0.006	H-1→LUMO (57%), HOMO→L+3 (15%)
330	0.011	H-1→LUMO (39%), HOMO→L+3 (33%)
321	0.012	HOMO→L+3 (17%), HOMO→L+5 (20%), HOMO→L+9 (20%), HOMO→L+11 (24%)
317	0.002	HOMO→L+4 (90%)
313	0.027	HOMO→L+6 (16%), HOMO→L+7 (43%), HOMO→L+8 (13%), HOMO→L+11 (14%)
310	0.350	H-2→LUMO (81%)
309	0.065	HOMO→L+6 (65%), HOMO→L+7 (13%)
306	0.133	HOMO→L+6 (10%), HOMO→L+11 (11%), HOMO→L+13 (52%)

Table S 8 Atomic coordinates of **SQPTZ-F** at the fundamental state after geometry optimization

Atom	X (Å)	Y (Å)	Z (Å)
C	-1.2573	0.07647	-0.16598
C	-1.4838	-0.68106	1.16237
C	-0.54594	-1.27453	2.00095
H	0.51478	-1.24387	1.76757
C	-0.98641	-1.91368	3.16746
H	-0.26173	-2.37947	3.83038
C	-2.34915	-1.95432	3.48788
H	-2.67519	-2.45386	4.39661
C	-3.29296	-1.35336	2.64953
H	-4.34981	-1.38264	2.90407
C	-2.85402	-0.71518	1.48629
C	-3.60355	-0.00135	0.44329

C	-4.97369	0.24542	0.30738
H	-5.68166	-0.11641	1.04911
C	-5.42295	0.96856	-0.80134
H	-6.48492	1.16841	-0.92012
C	-4.51621	1.43882	-1.76121
H	-4.87972	2.00027	-2.61801
C	-3.14463	1.19039	-1.62461
H	-2.44317	1.55543	-2.37093
C	-2.6953	0.47086	-0.52155
C	-0.35688	1.30138	0.05328
C	-0.87192	2.52292	0.50887
H	-1.94065	2.61792	0.67132
C	-0.03688	3.60719	0.77227
H	-0.45595	4.53977	1.13967
C	1.3396	3.49251	0.56694
H	2.00357	4.32882	0.76732
C	1.86584	2.29682	0.07861
C	1.0271	1.19299	-0.16132
C	-0.63453	-0.84309	-1.22876
C	-1.423	-1.69134	-2.02053
H	-2.50112	-1.67619	-1.89528
C	-0.85484	-2.55473	-2.9548
H	-1.49019	-3.20649	-3.54813
C	0.53324	-2.56411	-3.12901
H	0.99134	-3.21248	-3.87142
C	1.33401	-1.72457	-2.36239
H	2.40943	-1.70952	-2.50887
C	0.76101	-0.87929	-1.39604
C	2.83278	-0.45647	-0.10309
C	3.05437	-1.79789	0.24905
H	2.26578	-2.52764	0.09736
C	4.28405	-2.20072	0.77097
H	4.43833	-3.24696	1.02129
C	5.30096	-1.26674	0.98755
H	6.25657	-1.5764	1.40126
C	5.07477	0.07665	0.68373
H	5.84499	0.82068	0.86849
C	3.85661	0.47997	0.12774
S	3.59707	2.181	-0.33626
N	1.58914	-0.01805	-0.63465

No imaginary frequency

Table S 9 Atomic coordinates of **SQPTZ-F** at the first triplet state after geometry optimization

Atom	X (Å)	Y (Å)	Z (Å)
C	-1.24123	0.09526	-0.18111

C	-1.47903	-0.67462	1.1385
C	-0.57293	-1.2593	1.98428
H	0.4939	-1.2223	1.78024
C	-1.03601	-1.92501	3.15748
H	-0.3216	-2.38966	3.83022
C	-2.43425	-1.98465	3.45739
H	-2.75622	-2.50136	4.35825
C	-3.36729	-1.40179	2.63381
H	-4.42713	-1.44737	2.86877
C	-2.91589	-0.715	1.43841
C	-3.61678	-0.02586	0.45794
C	-5.03381	0.23499	0.2978
H	-5.74476	-0.14596	1.02573
C	-5.45643	0.97026	-0.78534
H	-6.51607	1.17464	-0.91866
C	-4.52902	1.4775	-1.74819
H	-4.89229	2.05417	-2.5934
C	-3.13242	1.22908	-1.60705
H	-2.43796	1.61911	-2.34755
C	-2.68065	0.49811	-0.53812
C	-0.33294	1.31072	0.05297
C	-0.84273	2.53094	0.51699
H	-1.91182	2.6307	0.67455
C	-0.00245	3.60816	0.79429
H	-0.41736	4.54016	1.16788
C	1.37432	3.48578	0.59689
H	2.04268	4.31543	0.81004
C	1.89632	2.29047	0.1016
C	1.05194	1.19503	-0.15388
C	-0.61772	-0.81936	-1.24745
C	-1.40866	-1.65472	-2.04981
H	-2.48731	-1.63186	-1.92984
C	-0.84248	-2.51476	-2.98889
H	-1.47939	-3.15702	-3.59089
C	0.54628	-2.53401	-3.15496
H	1.0033	-3.18064	-3.89957
C	1.35022	-1.70728	-2.3768
H	2.42646	-1.69976	-2.51799
C	0.77873	-0.86547	-1.40718
C	2.84444	-0.46806	-0.09645
C	3.05321	-1.81393	0.24653
H	2.26013	-2.53622	0.08304
C	4.2757	-2.23015	0.77479
H	4.42028	-3.27951	1.01779
C	5.29786	-1.30564	1.0069

H	6.24787	-1.62585	1.42544
C	5.08402	0.04187	0.71243
H	5.85828	0.77855	0.90934
C	3.87329	0.45886	0.15035
S	3.62982	2.16575	-0.30119
N	1.60861	-0.01597	-0.63414

Table S 10 Atomic coordinates of **SQPTZ-2,7-F(POPh<sub>2</sub>)<sub>2</sub>** at the fundamental state after geometry optimization

Atom	X (Å)	Y (Å)	Z (Å)
C	0.42325	0.04846	1.6398
C	0.30795	-1.21368	2.08501
C	-0.13342	-1.99926	1.08982
C	-0.30914	-1.25843	-0.01587
C	0.02271	0.19904	0.19135
C	0.8641	1.0252	2.44304
C	1.20391	0.72517	3.70824
C	1.07252	-0.53633	4.1571
C	0.62507	-1.51478	3.35153
C	-0.38708	-3.31499	1.06771
C	-0.81423	-3.87394	-0.07787
C	-0.98905	-3.13351	-1.18769
C	-0.73486	-1.81476	-1.15716
C	1.11918	0.65075	-0.72163
C	0.82805	1.34956	-1.84923
P	-1.56148	-3.89862	-2.73708
P	1.82806	2.05094	4.78822
N	-0.37819	1.73785	-2.14106
C	-1.28254	1.72261	-1.20412
C	-1.17042	1.06114	-0.03045
C	1.92516	1.54832	-2.61804
C	2.35175	0.19024	-0.4308
C	3.39909	0.42555	-1.22316
C	3.16975	1.12812	-2.33324
S	1.91534	2.56808	-4.10297
C	-2.37339	2.53334	-1.22168
C	-3.33779	2.57212	-0.28991
C	-3.24269	1.79149	0.78838
C	-2.1368	1.05115	0.90825
C	0.13869	2.5003	-4.339
C	-0.69549	2.14662	-3.33634
C	3.26426	2.97143	4.03106
C	2.75151	1.52789	6.30502
C	-0.23367	2.8837	-5.57354
C	-1.52276	2.8882	-5.92519

C	-2.39878	2.4521	-5.01701
C	-1.97289	2.07793	-3.80011
O	-3.03664	-3.86677	-2.91602
C	-0.98521	-5.65427	-2.95346
C	-0.81248	-3.22611	-4.29566
C	-1.59536	-2.71789	-5.26288
C	-1.05229	-2.23844	-6.39286
C	0.27817	-2.26738	-6.56425
C	0.30117	-5.91542	-3.24454
C	0.72233	-7.18115	-3.39105
C	-0.13697	-8.19873	-3.23058
C	-1.41747	-7.94555	-2.92116
C	-1.83845	-6.67858	-2.78155
C	3.75917	0.64431	6.19886
C	4.44161	0.25715	7.2878
C	4.12175	0.75343	8.49256
C	3.63156	4.17396	4.50612
C	4.66974	4.82953	3.96362
C	5.3521	4.28412	2.94514
O	0.81296	3.08522	5.11671
C	1.06335	-2.77889	-5.60396
C	0.51917	-3.25811	-4.47443
C	4.99664	3.07922	2.47405
C	3.95938	2.42435	3.01863
C	3.11899	1.63789	8.60401
C	2.43743	2.02407	7.51392
H	0.95178	2.04906	2.04582
H	1.33903	-0.7888	5.19694
H	0.53405	-2.54371	3.73383
H	-0.24664	-3.93849	1.96469
H	-1.01968	-4.95762	-0.09722
H	-0.86406	-1.17947	-2.04667
H	2.54199	-0.42286	0.46492
H	4.40634	0.05369	-0.97427
H	4.03219	1.34968	-2.98551
H	-2.51894	3.31532	-1.98707
H	-4.1909	3.26559	-0.38546
H	-4.01772	1.79968	1.5718
H	-2.04329	0.43492	1.81713
H	0.50474	3.19386	-6.33309
H	-1.84329	3.17919	-6.93851
H	-3.46103	2.35132	-5.29946
H	-2.78659	1.60076	-3.22671
H	-2.6912	-2.69041	-5.14273
H	-1.69989	-1.82264	-7.18295

H	0.72478	-1.87536	-7.49324
H	1.03036	-5.09725	-3.36428
H	1.77835	-7.38553	-3.63464
H	0.20987	-9.2394	-3.34343
H	-2.12326	-8.78087	-2.77787
H	-2.89347	-6.49564	-2.51939
H	4.03817	0.22536	5.21753
H	5.26642	-0.4689	7.19277
H	4.68197	0.43645	9.38801
H	3.08823	4.63704	5.3464
H	4.96477	5.81689	4.35687
H	6.20602	4.8218	2.50031
H	2.15689	-2.80816	-5.74488
H	1.18192	-3.67977	-3.701
H	5.55964	2.62493	1.64135
H	3.6926	1.43189	2.61981
H	2.85557	2.04836	9.59333
H	1.61886	2.75304	7.63053

No imaginary frequency

Table S 11 Atomic coordinates of **SQPTZ-2,7-F(POPh<sub>2</sub>)<sub>2</sub>** at the first triplet state after geometry optimization

Atom	X (Å)	Y (Å)	Z (Å)
C	1.71067	0.50331	-0.05876
C	1.63869	1.82896	-0.58787
C	0.27879	2.17884	-0.83164
C	-0.57706	1.09397	-0.45798
C	0.29305	-0.07778	0.07989
C	2.90511	-0.09154	0.26954
C	4.12718	0.6265	0.08568
C	4.05965	1.9473	-0.42832
C	2.8547	2.5473	-0.76473
C	-0.31869	3.35364	-1.36656
C	-1.69512	3.41593	-1.5186
C	-2.54053	2.33757	-1.15357
C	-1.94148	1.15983	-0.6058
C	-0.04942	-0.39373	1.5373
C	-1.02075	-1.37238	1.85037
P	-4.30907	2.55634	-1.35715
P	5.64835	-0.22958	0.51001
N	-1.60491	-2.11191	0.80872
C	-0.84124	-2.30628	-0.38767
C	0.09653	-1.33178	-0.76569
C	-1.3814	-1.61578	3.19938
C	0.52832	0.31008	2.58768

C	0.17583	0.06552	3.92486
C	-0.77103	-0.89657	4.2365
S	-2.52503	-2.86964	3.64358
C	-0.98142	-3.50626	-1.10802
C	-0.23497	-3.70683	-2.26287
C	0.65594	-2.71692	-2.69038
C	0.82672	-1.55476	-1.93849
C	-3.44386	-3.01602	2.16139
C	-2.90809	-2.61881	0.9102
C	6.89563	1.05491	0.93504
C	6.30176	-1.03348	-1.01568
C	-4.7328	-3.57295	2.23353
C	-5.50671	-3.69372	1.08994
C	-5.00812	-3.23732	-0.14384
C	-3.73104	-2.7133	-0.23585
O	-4.67716	3.82175	-2.0944
C	-5.10474	2.54334	0.30673
C	-4.95319	1.03521	-2.18613
C	-6.30235	0.67009	-2.04982
C	-6.83336	-0.38852	-2.79094
C	-6.02082	-1.0976	-3.682
C	-5.15563	1.42008	1.14705
C	-5.73246	1.50754	2.41605
C	-6.26733	2.72101	2.86161
C	-6.22591	3.84313	2.02934
C	-5.64989	3.75452	0.75892
C	5.98967	-0.58381	-2.30694
C	6.51666	-1.23121	-3.42926
C	7.3541	-2.33874	-3.26965
C	7.07356	1.34281	2.29719
C	7.99206	2.31453	2.70031
C	8.74457	3.00737	1.74646
O	5.48398	-1.24523	1.61881
C	-4.67702	-0.73998	-3.82929
C	-4.14835	0.32123	-3.08774
C	8.58166	2.71831	0.38897
C	7.66463	1.74314	-0.01486
C	7.65936	-2.80096	-1.98502
C	7.13525	-2.15306	-0.86421
H	2.94408	-1.09395	0.68969
H	4.97652	2.51953	-0.54967
H	2.84382	3.56529	-1.14594
H	0.29874	4.19655	-1.66667
H	-2.15425	4.30678	-1.9389
H	-2.57116	0.32012	-0.32269

H	1.26586	1.0697	2.35909
H	0.64607	0.639	4.71755
H	-1.05609	-1.08842	5.26665
H	-1.65159	-4.28118	-0.75252
H	-0.33746	-4.63597	-2.81576
H	1.2397	-2.86177	-3.59484
H	1.54688	-0.80751	-2.25049
H	-5.12363	-3.88027	3.19935
H	-6.50843	-4.10676	1.1565
H	-5.63157	-3.26604	-1.0315
H	-3.36665	-2.33875	-1.18469
H	-6.94465	1.22228	-1.36873
H	-7.88332	-0.65083	-2.68276
H	-6.43671	-1.91278	-4.26999
H	-4.7583	0.46652	0.80783
H	-5.7713	0.62861	3.05574
H	-6.7176	2.78856	3.84908
H	-6.64623	4.78757	2.36662
H	-5.62175	4.61703	0.09865
H	5.32264	0.26481	-2.43762
H	6.26898	-0.87291	-4.42585
H	7.76224	-2.84358	-4.1421
H	6.49905	0.78739	3.03365
H	8.12496	2.52707	3.75843
H	9.46078	3.76299	2.06024
H	-4.04359	-1.27565	-4.53278
H	-3.10745	0.60516	-3.21686
H	9.17271	3.24526	-0.35631
H	7.56181	1.51206	-1.072
H	8.30225	-3.66867	-1.85694

## 7 Single layer Phosphorescent OLED characteristics

The architecture of the single layer devices is the following: ITO/PEDOT:PSS (40 nm)/Emissive layer (host matrix + red or green or blue phosphorescent guest 10%, 100 nm)/LiF (1.2 nm)/Al (100 nm).

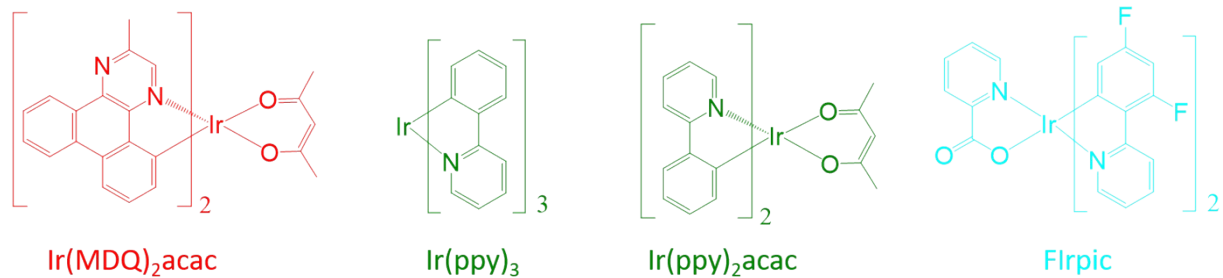
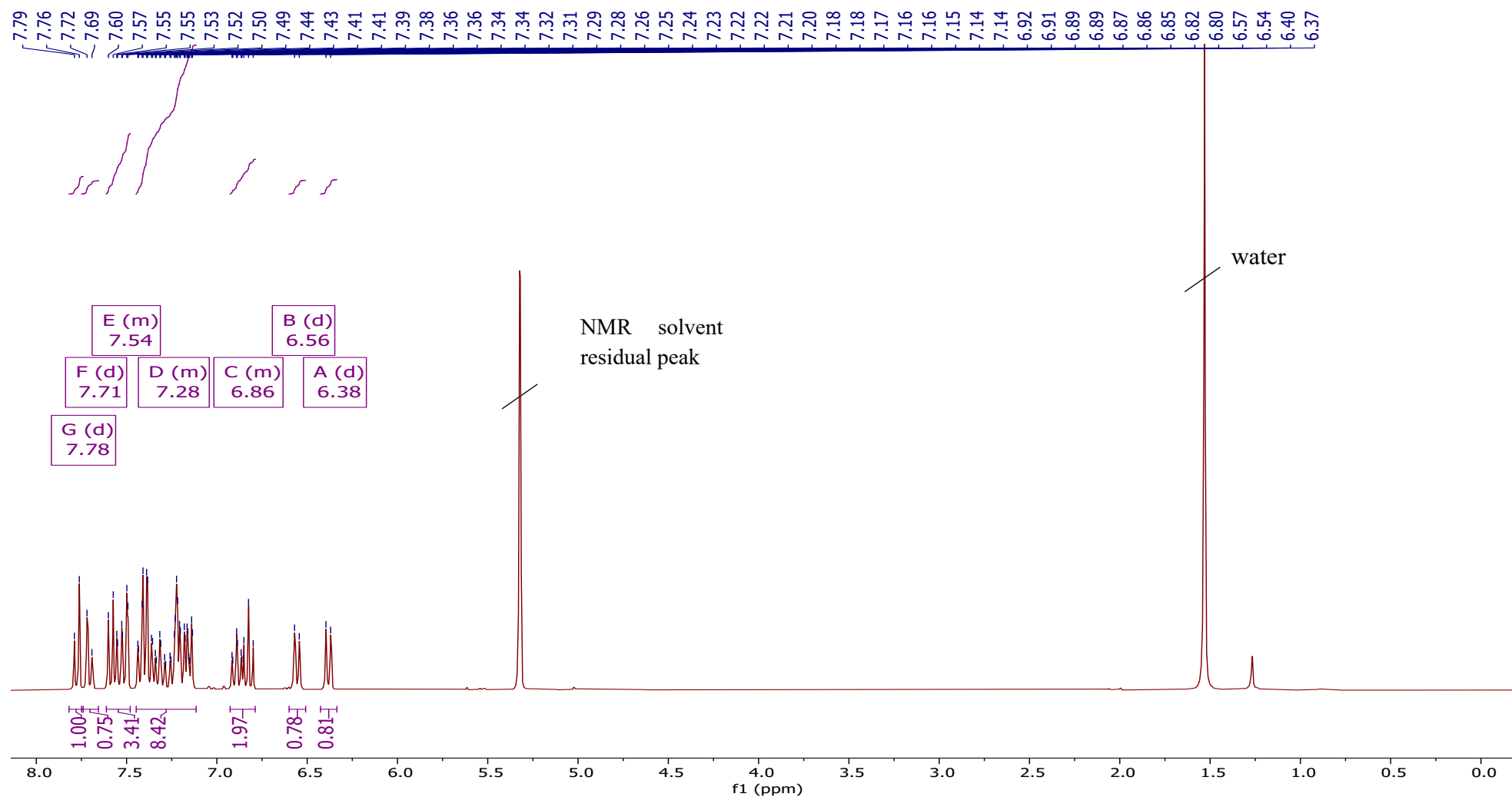


Chart 1 Molecular structures of the phosphorescent emitters used

## 8 Copy of NMR spectra

### 8.1 SQPTZ-2,7-FBr<sub>2</sub> – <sup>1</sup>H – CD<sub>2</sub>Cl<sub>2</sub>



*Figure S 15 SQPTZ-2,7-FBr<sub>2</sub> – <sup>1</sup>H – CD<sub>2</sub>Cl<sub>2</sub>*

8.2 SQPTZ-2,7-FBr<sub>2</sub> – <sup>13</sup>C – CD<sub>2</sub>Cl<sub>2</sub>

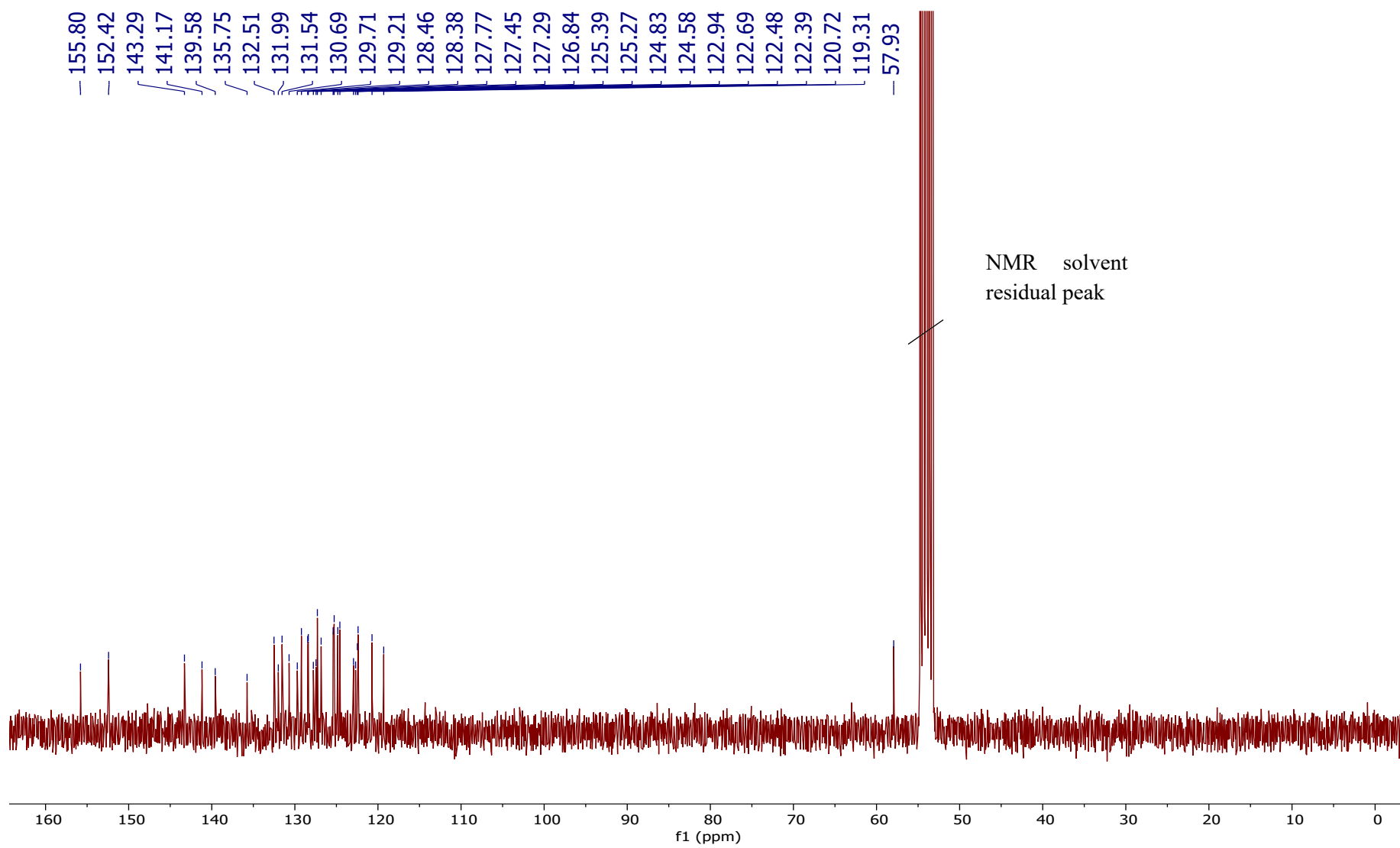


Figure S 16 SQPTZ-2,7-FBr<sub>2</sub> – <sup>13</sup>C – CD<sub>2</sub>Cl<sub>2</sub>

8.3 SQPTZ-2,7-FBr<sub>2</sub> – <sup>13</sup>C – DEPT135 – CD<sub>2</sub>Cl<sub>2</sub>

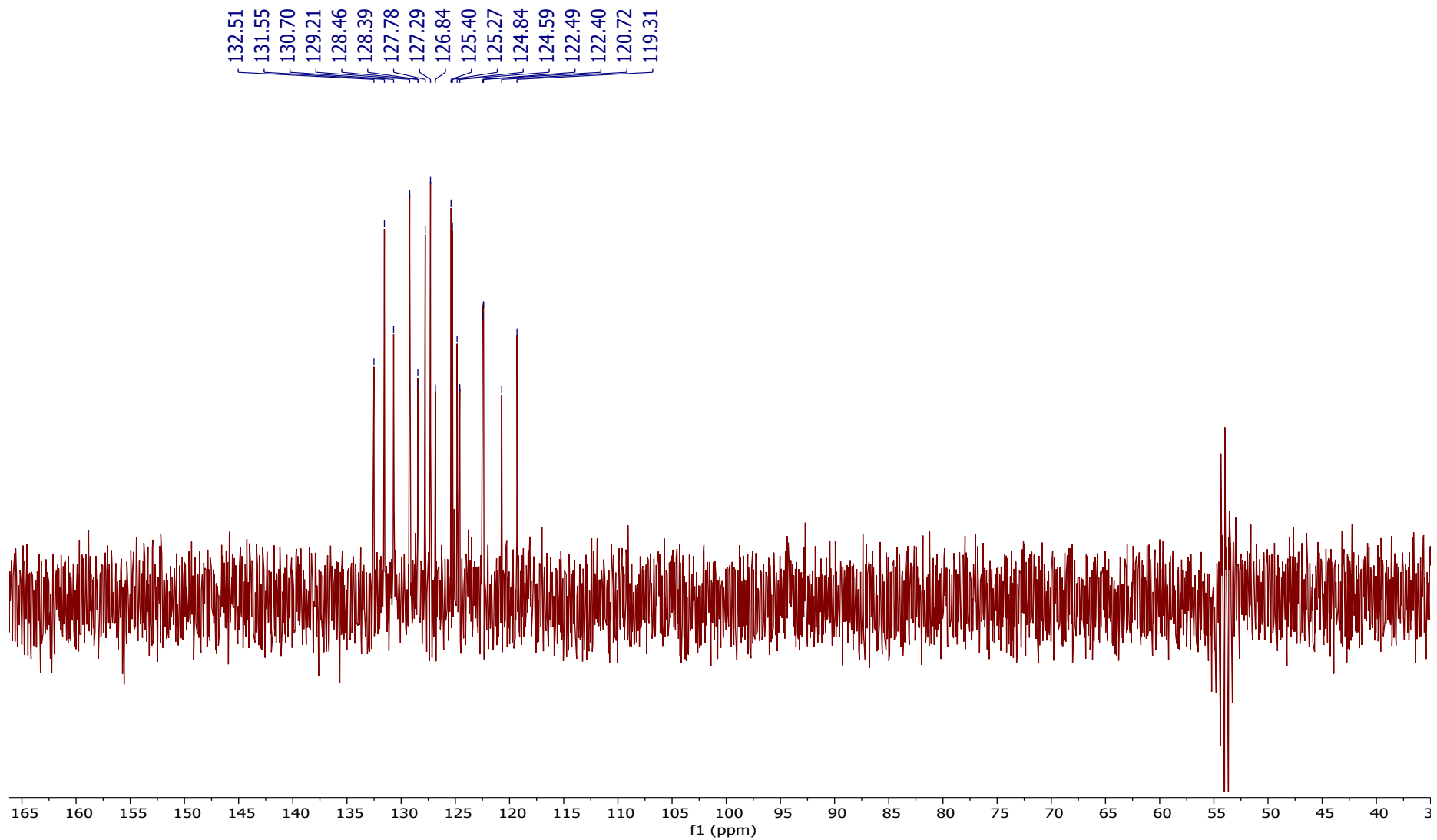


Figure S 17 SQPTZ-2,7-FBr<sub>2</sub> – <sup>13</sup>C – DEPT135 – CD<sub>2</sub>Cl<sub>2</sub>

8.4 SQPTZ-2,7-F(POPh<sub>2</sub>)<sub>2</sub> – <sup>1</sup>H – CD<sub>2</sub>Cl<sub>2</sub>

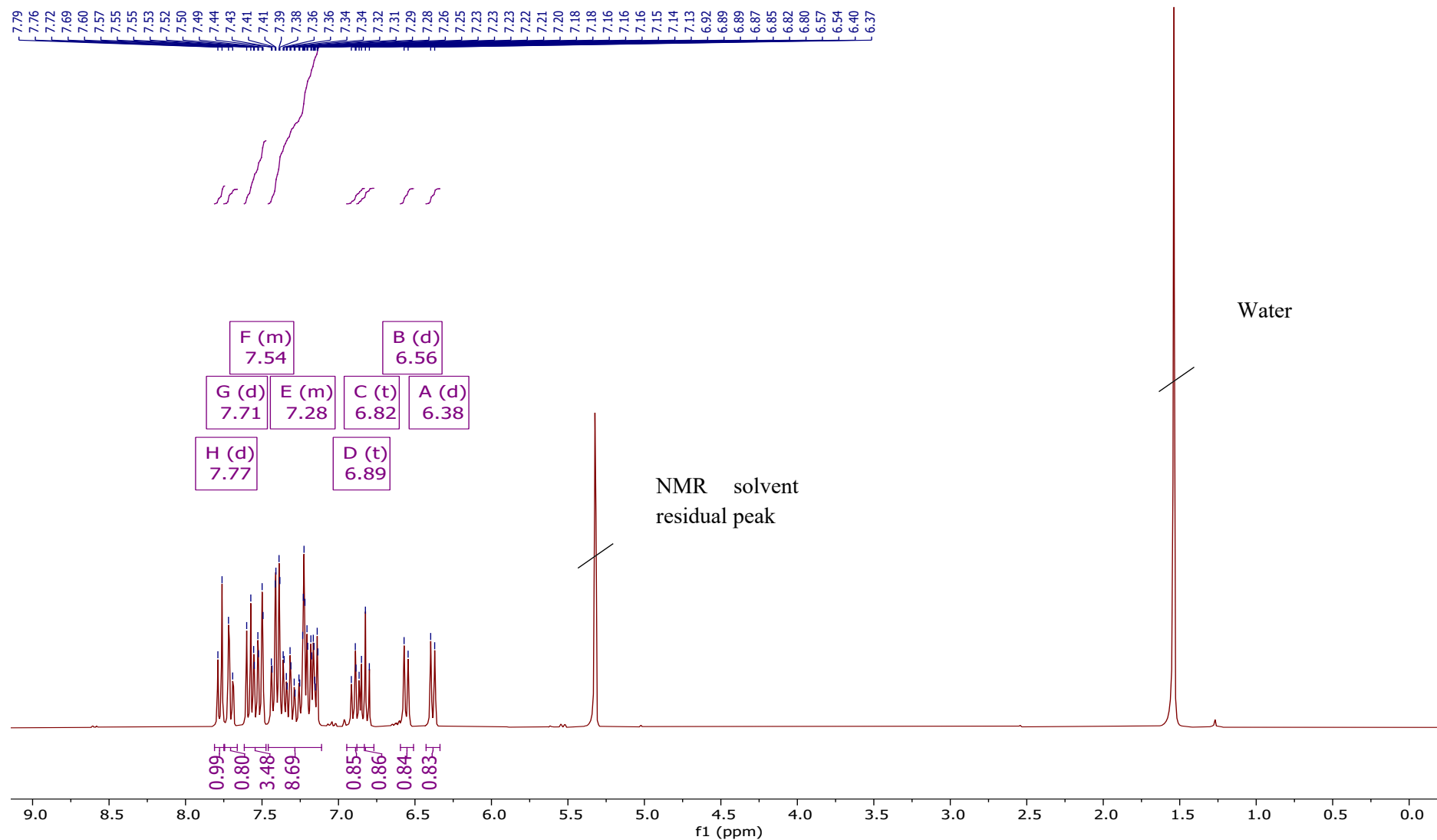


Figure S 18 SQPTZ-2,7-F(POPh<sub>2</sub>)<sub>2</sub> – <sup>1</sup>H – CD<sub>2</sub>Cl<sub>2</sub>

8.5 SQPTZ-2,7-F(POPh<sub>2</sub>)<sub>2</sub> - <sup>13</sup>C - CD<sub>2</sub>Cl<sub>2</sub>

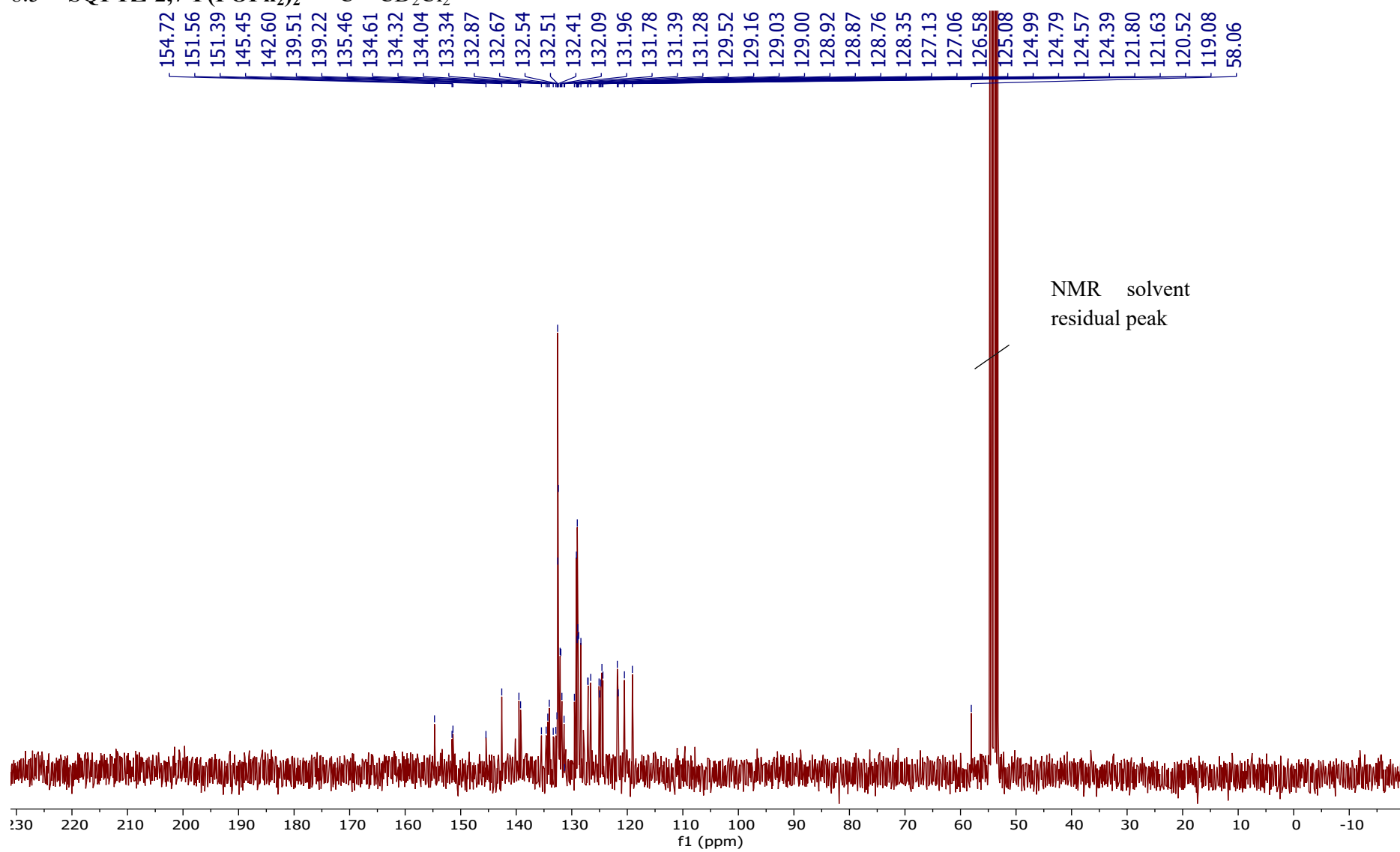


Figure S 19 SQPTZ-2,7-F(POPh<sub>2</sub>)<sub>2</sub> - <sup>13</sup>C - CD<sub>2</sub>Cl<sub>2</sub>

8.6 SQPTZ-2,7-F(POPh<sub>2</sub>)<sub>2</sub> – <sup>13</sup>C – DEPT 135 – CD<sub>2</sub>Cl<sub>2</sub>

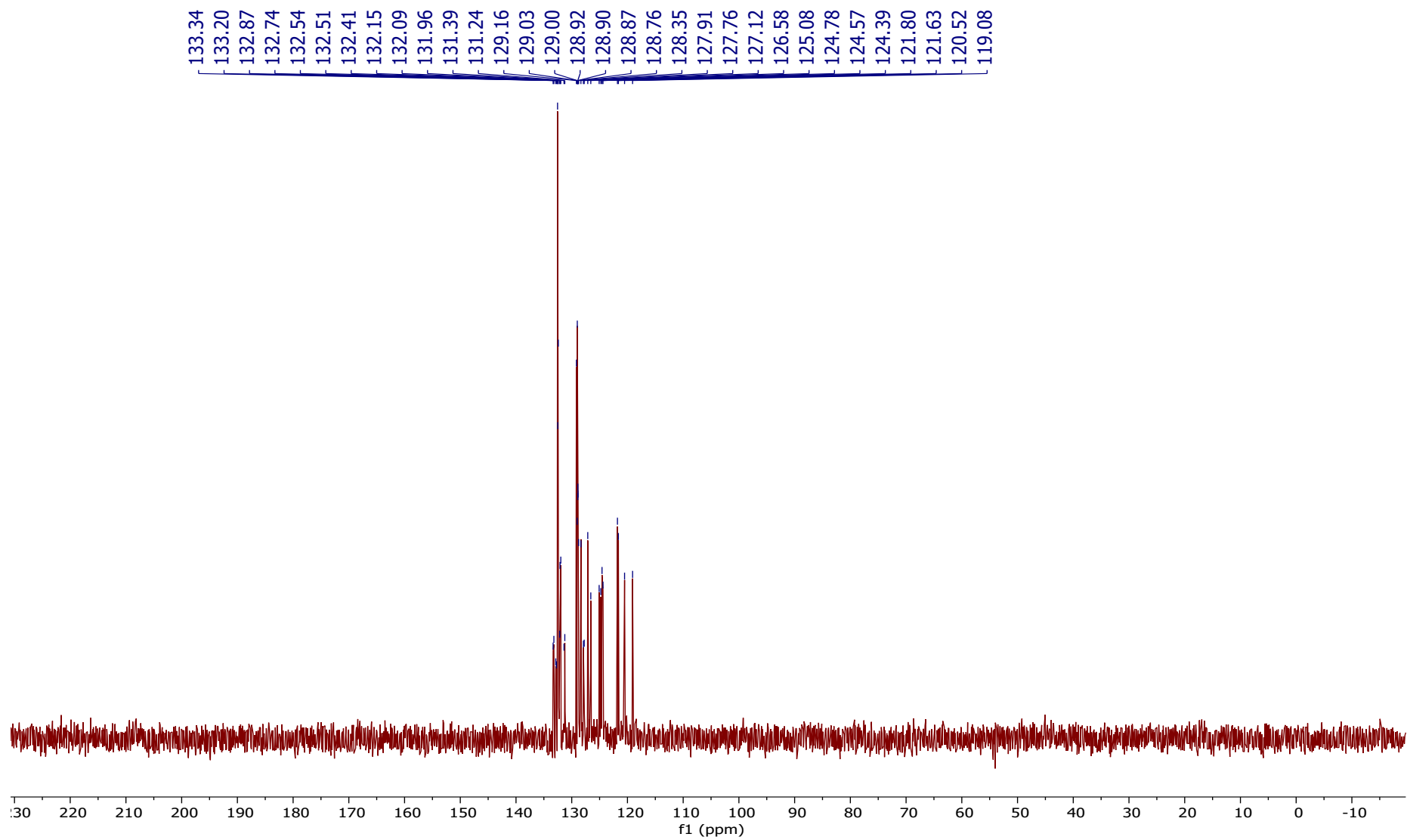


Figure S 20 SQPTZ-2,7-F(POPh<sub>2</sub>)<sub>2</sub> – <sup>13</sup>C – DEPT 135 – CD<sub>2</sub>Cl<sub>2</sub>

8.7 SQPTZ-2,7-F(POPh<sub>2</sub>)<sub>2</sub> – <sup>31</sup>P decoupled – CD<sub>2</sub>Cl<sub>2</sub>

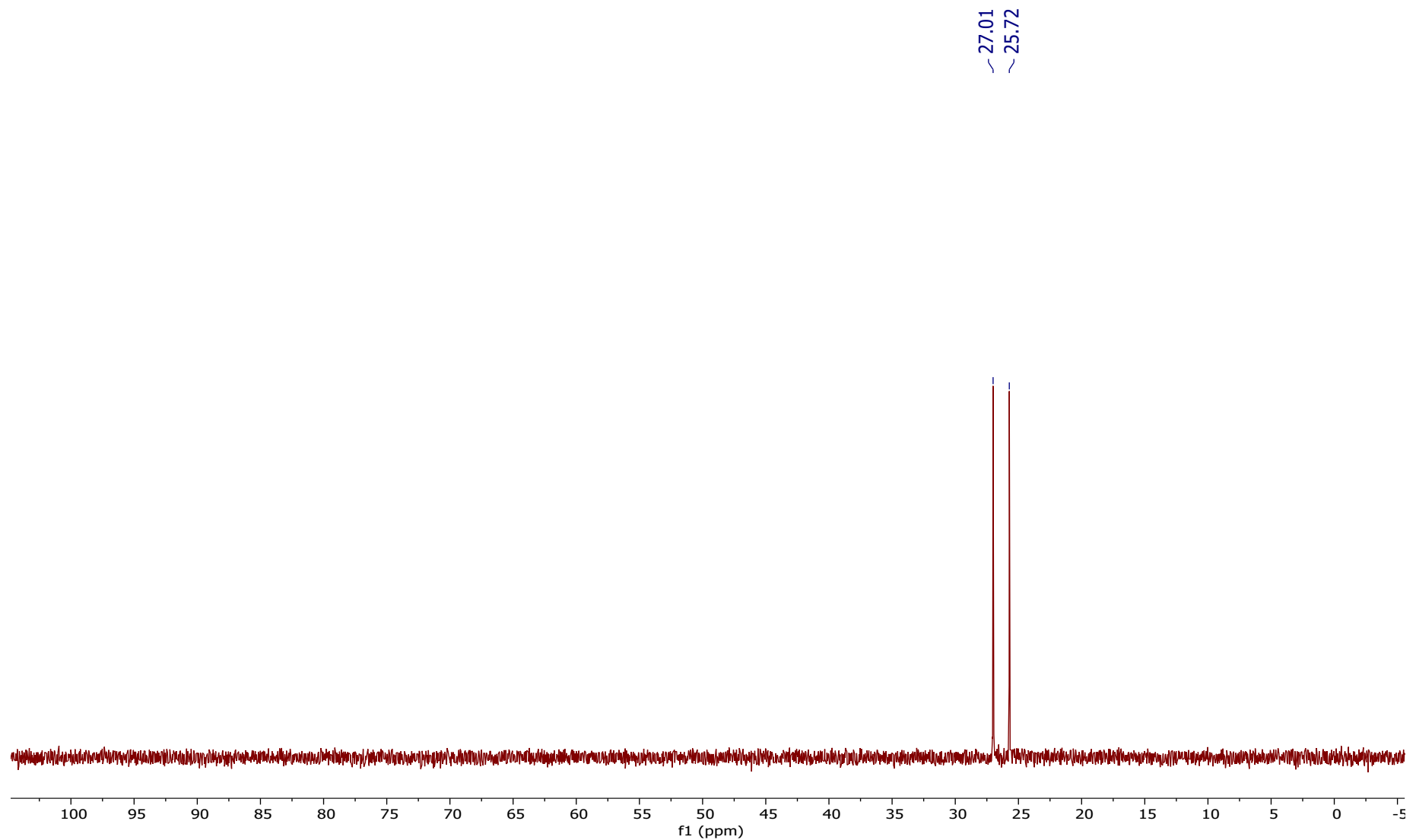


Figure S 21 SQPTZ-2,7-F(POPh<sub>2</sub>)<sub>2</sub> – <sup>31</sup>P decoupled – CD<sub>2</sub>Cl<sub>2</sub>

## 9 Copy of high resolution mass spectroscopy spectra

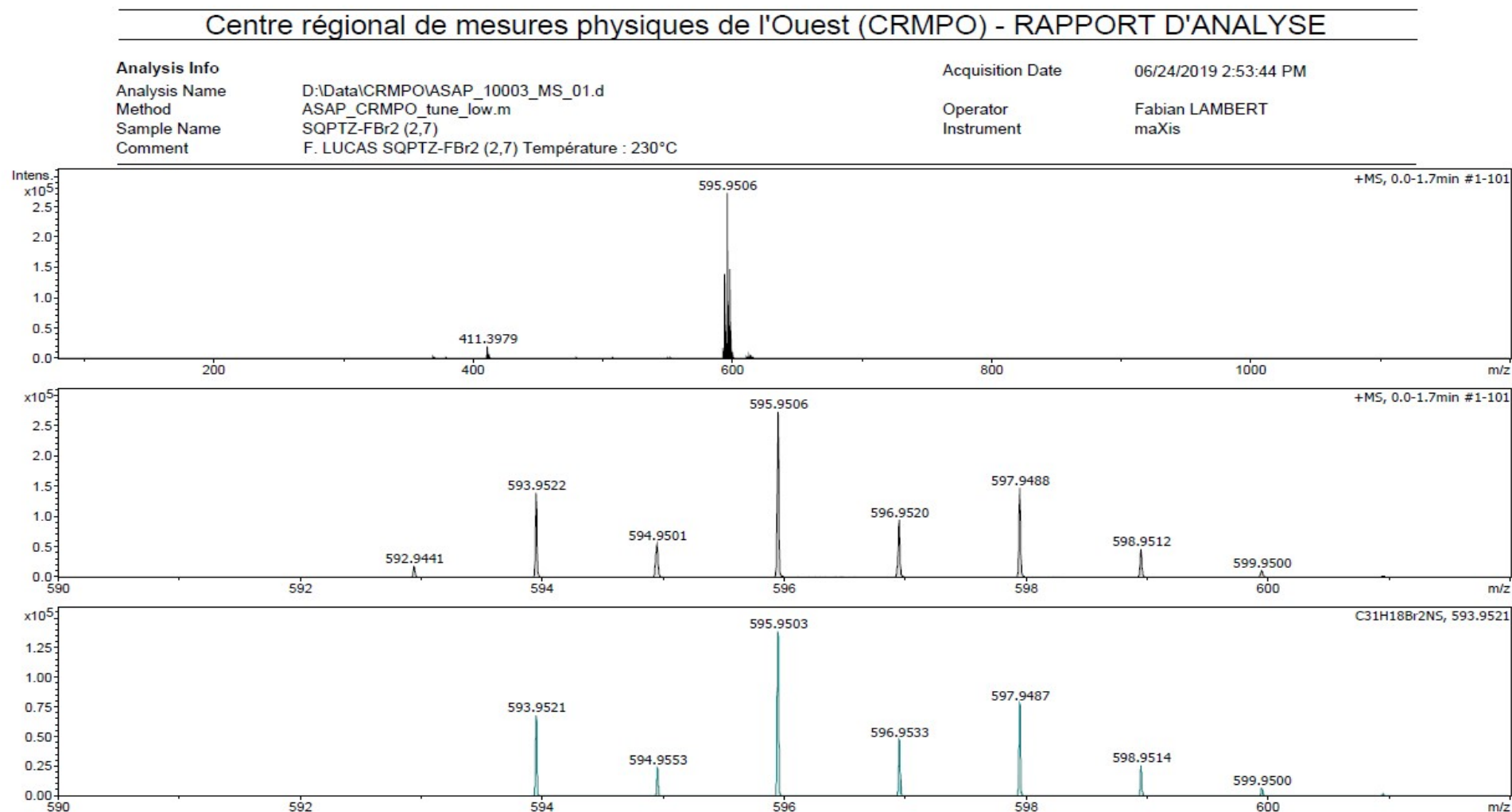


Figure S 22 HRMS spectrum of **SQPTZ-2,7-FBr<sub>2</sub>**

Centre régional de mesures physiques de l'Ouest (CRMPO) - RAPPORT D'ANALYSE

**Analysis Info**

Analysis Name D:\Data\CRMPO\ASAP\_9648\_MS\_01.d  
 Method ASAP\_CRMPO\_tune\_low.m  
 Sample Name SQPTZ-F(POPh<sub>2</sub>)<sub>2</sub>  
 Comment F. LUCAS SQPTZ-F(POPh<sub>2</sub>)<sub>2</sub> Température : 325°C

Acquisition Date

04/10/2019 4:04:40 PM

Operator  
Instrument

Fabian LAMBERT  
maXis

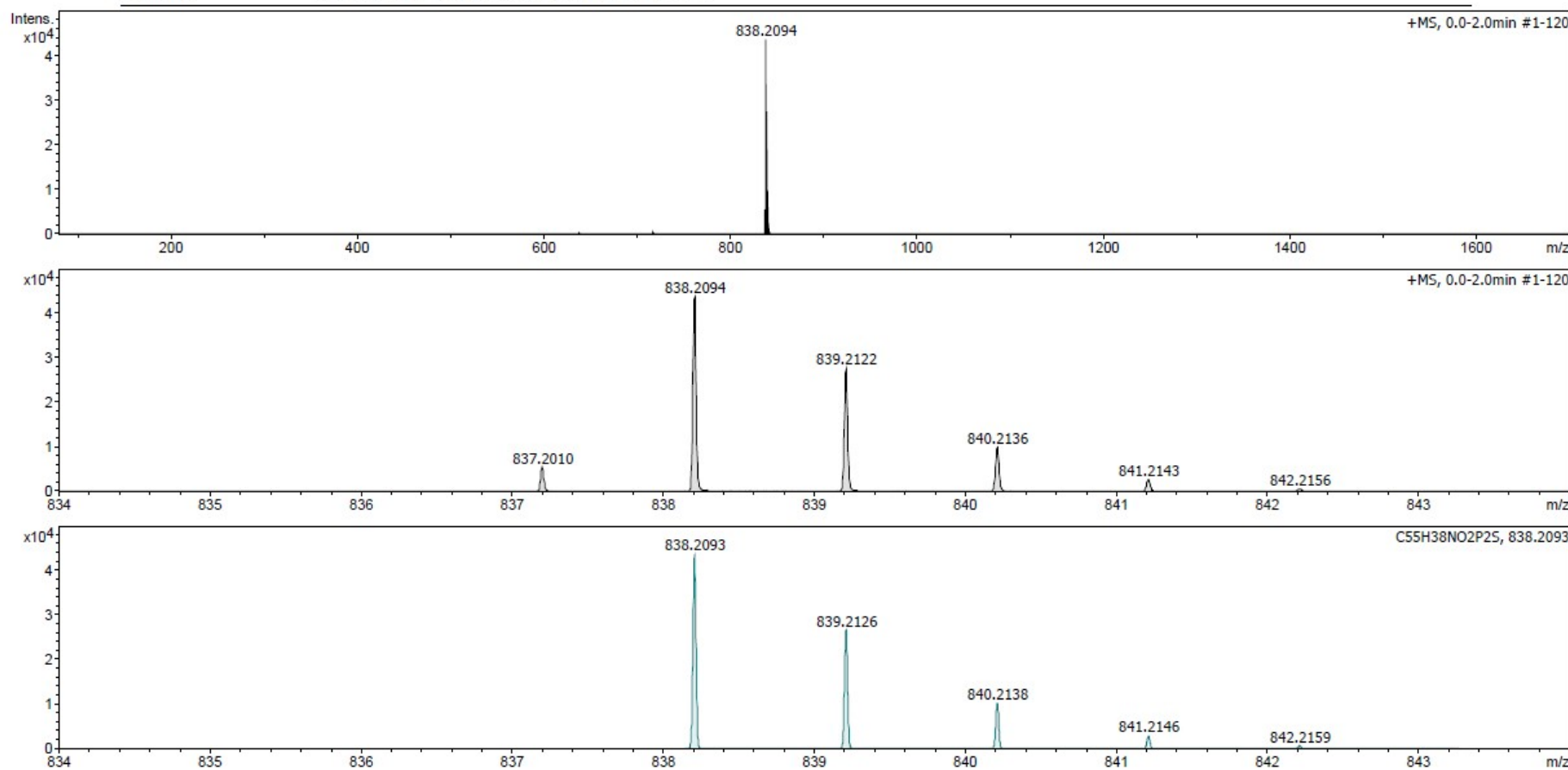


Figure S 23 HRMS spectrum of SQPTZ-2,7-F(POPh<sub>2</sub>)<sub>2</sub>

## 10 References

- [1] G. R. Fulmer, A. J. M. Miller, N. H. Sherden, H. E. Gottlieb, A. Nudelman, B. M. Stoltz, J. E. Bercaw, K. I. Goldberg, *Organomet.* **2010**, *29*, 2176-2179.
- [2] E. Lippert, *Zeitschrift für Naturforschung* **1955**, 541.
- [3] Y. Ooshika, *J. Phys. Soc. Jpn.* **1954**, *9*, 594.
- [4] N. Mataga, Y. Kaifu, M. Koiz, *Bull. Chem. Soc. Jpn.* **1956**, *29*, 456.
- [5] A. P. Kulkarni, C. J. Tonzola, A. Babel, S. A. Jenekhe, *Chem. Mater.* **2004**, *16*, 4556-4573.
- [6] aP. H. a. W. Kohn, *Phys. Rev.*, **136**, B864; bJ.-L. Calais, *Int. J. Quantum Chem.* **1993**, *47*, 101.
- [7] aA. D. Becke, *J. Phys. Chem.* **1993**, *98*, 1372; bA. D. Becke, *J. Phys. Chem.* **1993**, *98*, 5648; cA. D. Becke, *Phys. Rev. A* **1988**, *38*, 3098.
- [8] Y. W. a. R. G. P. Lee C., *phys. rev. B* **1988**, *37*, 785.
- [9] G. W. T. M. J. Frisch, H. B. Schlegel, G. E. Scuseria, M. A. Robb, J. R. Cheeseman, G. Scalmani, V. Barone, B. Mennucci, G. A. Petersson, H. Nakatsuji, M. Caricato, X. Li, H. P. Hratchian, A. F. Izmaylov, J. Bloino, G. Zheng, J. L. Sonnenberg, M. Hada, M. Ehara, K. Toyota, R. Fukuda, J. Hasegawa, M. Ishida, T. Nakajima, Y. Honda, O. Kitao, H. Nakai, T. Vreven, J. A. J. Montgomery, J. E. Peralta, F. Ogliaro, M. Bearpark, J. J. Heyd, E. Brothers, K. N. Kudin, V. N. Staroverov, T. Keith, R. Kobayashi, J. Normand, K. Raghavachari, A. Rendell, J. C. Burant, S. S. Iyengar, J. Tomasi, M. Cossi, N. Rega, J. M. Millam, M. Klene, J. E. Knox, J. B. Cross, V. Bakken, C. Adamo, J. Jaramillo, R. Gomperts, R. E. Stratmann, O. Yazyev, A. J. Austin, R. Cammi, C. Pomelli, J. W. Ochterski, R. L. Martin, K. Morokuma, V. G. Zakrzewski, G. A. Voth, P. Salvador, J. J. Dannenberg, S. Dapprich, A. D. Daniels, O. Farkas, J. B. Foresman, J. V. Ortiz, J. Cioslowski, D. J. Fox, **2010**, Gaussian 09, Revision B.01, Gaussian, Inc., Wallingford CT, 2010.
- [10] C. Poriel, J. Rault-Berthelot, S. Thiery, C. Quinton, O. Jeannin, U. Biapo, D. Tondelier, B. Geffroy, *Chem. Eur. J.* **2016**, *22*, 17930-17935.